Opto-Electronics Review 28 (2020) 15-34

PAN POLISH ACADEMY OF SCIENCES

Opto-Electronics Review

journal homepage: http://journals.pan.pl/opelre

Numerical procedures and their practical application in PV module analyses. Part III: parameters of atmospheric transparency – determining and correlations

T. Rodziewicz[1*], M. Rajfur[1*]

[1] Institute of Environmental Engineering and Biotechnology, University of Opole, 6a Kard. B. Kominka St., 45-032 Opole, Poland

Article info

Article history:
Received 19 Nov. 2019
Received in revised form 04 March 2020
Accepted 10 March 2020

Keywords:
solar radiation spectrum, sky clearness index, diffused component content index, solar energy, photovoltaics

Abstract

The presented article examines aspects of a PV module testing using natural sunlight in outdoor conditions. The article discusses the physical sense of indexes: atmosphere purity, diffused component content, beam clear sky index. Procedures for their determination are given in relation to both instantaneous and daily values. Their close connection with the values of solar irradiance spectral distribution such as Average Photon Energy and Useful Fraction is demonstrated, as well as their usefulness in module testing in outdoor conditions. Their influence on the conversion of modules made from various absorbers and various technologies is demonstrated.

1. Introduction

It is quite difficult to estimate the usefulness of modules (i.e., maintaining their standard parameters) made of different absorbers using different technologies in areas located in higher geographical latitudes. This is due to the fact, that such areas are characterised by a considerable variability in climate conditions. There are considerable differences in yearly distributions of average environment temperatures, irradiance and average energy of photons of the solar irradiance spectrum. The annual distribution of environment temperatures and irradiance can be determined in a simple, unambiguous and cheap way; problems arise during preparation of the annual solar irradiance spectrum distribution. Performance of an analysis of solar irradiation spectrum distribution and spectral response of the applied PV modules' correspondence require the use of expensive and complex measuring equipment. In this context, application of purity/transparency indexes and the respective index of a diffused component content in estimating the modules' usefulness, made from various absorbers and in various technologies for operation in outdoor conditions, becomes simpler. The presented article was prepared using measurement data generated in two research centres – AGH University of Science and Technology in Krakow and Laboratorium SolarLab in Wroclaw Technical University (both located in Poland). The basic studies were carried out using the measurement data from SolarLab at Wroclaw Technical University, whereas data generated at AGH Krakow were treated as supplementary[1], i.e., comparative. A precise description of the lab measuring stations used in the studies – at AGH Krakow and SolarLab at Wroclaw Technical University – was Refs. 1, 2 and in Refs. 3, 4, respectively.

The presented article is the third one of a series of the interrelated articles which discuss the issue of PV modules and measurements, and testing cells in outdoor conditions, i.e., with the use of natural sunlight. The first article contains an analysis of the theory and practice of measurements with the use of Air Mass and its

* Corresponding author: trodziewicz@wp.pl, mrajfur@o2.pl
phone: +48 77 401 60 42, fax: +48 77 401 60 50

[1] Considering the occurrence of shade on the measuring systems in SolarLab early morning (i.e., for very low angles of solar irradiance), it was necessary to supplement the data from the AGH Krakow measuring system where this phenomenon did not occur. This applies particularly to the presentations of instantaneous relations of the values of Useful Fraction and Average Photon Energy with the value of Air Mass.

https://doi.org/10.24425/opelre.2020.132499

determination [5]. The second one refers to the theory and practice of measurements, with the use of such spectral parameters as Useful Fraction, Average Photon Energy and a connection was made with Air Mass [6].

This article includes a discussion on the physical sense of the indexes: atmosphere purity, diffuse component content, beam clear sky index. A very close relation of the indexes with the figures characterizing spectral distribution of solar irradiation was demonstrated. The above article was written as a guide for the aforementioned research with very extensive details of some leads and comments.

Nomenclature:

AM – Air Mass [-];
AM_p – the adjusted value of AM due to instantaneous fluctuations of atmospheric pressure [-];
$A_o(\lambda)$, $A_w(\lambda)$, $A_g(\lambda)$ – effective absorption coefficient of ozone, steam, gases mix (mainly O_2 and CO_2) [-];
APE – Average Photon Energy of solar radiation [eV];
B – bandwidth of the spectroradiometer [μm];
d – day number 1–365 (366);
E_0 – daily value of insolation energy [Wh/m^2];
$E_{0,H}(0)$ – daily irradiation energy on the Earth's surface in horizontal plane [Wh/m^2];
$E_{B,H}(0)$ – daily irradiation energy from direct component on the Earth's surface in horizontal plane [Wh/m^2];
$E_C(0)$ – mean daily value of insolation energy in a month in the upper atmosphere in the horizon [Wh/m^2];
$E_{ph}(\lambda)$ – photon energy with wavelength λ [J];
E_{POA} – daily value of insolation energy in the plane of array [Wh/m^2];
E_S – daily value of insolation energy from diffuse component [Wh/m^2];
$E_{S,H}(0)$ – daily irradiation energy from diffuse component on the Earth's surface on a horizontal surface [Wh/m^2];
$G_{0\,=}\,G_{0,H}$ – global solar irradiance in the plane of the horizon [W/m^2];
G_B (t) – irradiation beam in the plane of array [W/m^2];
$G_{B,H}$ (t) – beam irradiance/irradiation on a horizontal surface [W/m^2];
$G_{B,H0}$ (t) – extraterrestrial irradiation in the upper atmosphere in the horizon[W/m^2];
$G_{d\ external}$ – extraterrestrial irradiance/irradiation on a surface perpendicular to the solar beam [W/m^2];
G_{POA} – global irradiance in plane of array [W/m^2];
$G_{POA}(\lambda)$ – spectral irradiance G_{POA} [Wm^{-2}λm^{-1}];
$G_S = G_{S,0}$ – diffuse component in the plane of the horizon [W/m^2];
I_0 – solar constant (1367 ±7 W/m^2);
K_b – beam clear sky index – proportion between beam irradiance and extraterrestrial solar irradiance on a horizontal surface [-];
K_{b_day} – daily beam clear sky index;
$k_{s/o}$ – diffuse component content index of solar radiation [-];
k_{s/o_day} – daily diffuse component content index of solar radiation [-];
k_{Tm} – atmosphere clearness (transparency) index [-];
k_{Tm_day} – daily atmosphere clearness index [-];
LST – Local Solar Time [hh:mm];
m_o – optical masses of O_3 [-],
$Pm_{\_\text{in STC}}$ – a module power achieved in STC conditions [W_p];
$Pm(25°C)$ – a module power achieved at temperature of T_C=25°C [W_p];
$[Pm(25°C)/G_{POA}]_{norm}$ – standardised value of a PV module power for T_C = 25ºC for 1 W of the rate G_{POA} (standardisation is carried out up to the power of $P_{\text{min STC}}$ obtained in STC conditions, for 1 W of the rate G_{POA}) [-];
POA – Plane of Array;
SR (λ) – Spectral Response [A/W];
T_C – temperature of cells in a PV module [°C];
T_L – Linke turbidity factor [-];
$T_R(\lambda)$, $T_o(\lambda)$,$T_g(\lambda)$,$T_w(\lambda)$,$T_a(\lambda)$ – transmittance related to Rayleigh scattering, absorption by ozone, mix of gases (mainly O_2 and CO_2), by steam particles and extinction on aerosols [-];
UF – Useful Fraction [-];
w, w_o – content in atmosphere: steam [cm], ozone [atm-cm];
z – angle between a falling beam and normal to horizon [rad];
β – Angstrom turbidity coefficient [-];
λ_{cut} – limit wavelength measured by the equipment;
α_d – angle of the Earth's orbiting the Sun [rad];
ϕ_{ph} – photon spectral flux density [cm^{-2}s^{-1}μm^{-1}].

2. The spectrum structure of irradiation falling on the Earth's surface

The intensity of solar irradiation falling on the Earth's horizon, its structure (i.e., the content of a diffused component) and the shape of the radiation spectrum depend on instantaneous value of solar radiation intensity in the upper atmosphere, geographical location, atmosphere thickness through which light passes, solar radiation incidence angle, area profile and current meteorological conditions. The value of the radiation reaching the upper layers of the Earth's atmosphere (i.e., outside of the atmosphere) is variable due to the Earth's rotation around the Sun on an elliptical orbit. It fluctuates from 1.33 kW/m^2 in July, when the distance of the Earth to the Sun is the longest ($1.522\cdot10^8$ km) to 1.42 kW/m^2 in January, at a distance of $1.472\cdot10^8$ km [7]. Its mean value, at the average distance of the Earth from the Sun ($1.495\cdot10^8$ km) is called the solar constant I_0 and amounts to 1367±7 W/m^2 (WMO, Commission for Measurements and Observation Methods, 8th session, Mexico City, 1981).
Its instantaneous value was estimated by Spencer [8] in the following relation:

$$G_{d\ external}(\alpha_d) = I_0(1.00011 + 0.034221\cos\alpha_d + \\ +0.00128\sin\alpha_d + 0.000719\cos 2\alpha_d + 0.000077\sin 2\alpha_d). \quad (1)$$

The resolution of a component direct beam of solar irradiation on the Earth's surface ($G_B(t)$), its stream on the horizon plane ($G_{B,H}$) and its global value ($G_{0,H}$) depend on the instantaneous values of the following factors: atmosphere air mass (AM) value and beam clear sky index (K_b), as follows [8, 9]:

$$G_{B,H}(t) = K_b(t)\cdot[G_{d\ external}\cdot cos(z)] = K_b(t)\cdot G_{B,H0}(t), \quad (2)$$

$$G_{0,H}(t) = G_{B,H}(t) + G_{S,H}(t), \quad (3)$$

$$\alpha_d = 2\pi(d-1)/365. \quad (4)$$

Attenuation of irradiation from the upper atmosphere (AM0 type) during the passage through the Earth's atmosphere is the result of aerosol dispersion and absorption by various components of the atmosphere, mainly steam and such gases as ozone, carbon dioxide and oxygen. Some of them attenuate at a constant rate whereas others depend on the time and geographical location. The required minimum for the atmosphere characteristics includes turbidity parameters and steam content. Distribution of irradiation falling on the Earth's surface is the effect of the air and steam reaction in the atmosphere, due to absorption bandwidths of the solar irradiation spectrum. Additionally, together with the increase of humidity, steam condenses in aerosols and their value and refractive index change, as well as, in consequence, their ability to disperse irradiation. Atmospheric turbidity is the measure of attenuation of a direct irradiation beam by atmospheric aerosol. It includes quantitative influence, type and size of aerosol, as well as steam quantity and distribution in the atmosphere. It is commonly represented as an index. Three indexes in use are β, T_L, and B [10,11].

The passing of solar irradiation through the Earth's atmosphere is modelled as a product of reference irradiation beam with AM0 distribution falling in the upper atmosphere $G_{B,\,H0}(\lambda)$ [10,12–14] and transmittance functions which model physical phenomena [15–18]:

$$G_{B,H}(\lambda) = G_{B,\,H0}(\lambda) \cdot T_R(\lambda)T_a(\lambda)T_w(\lambda)T_o(\lambda)T_g(\lambda)\,, \quad (5)$$

$$T_R(\lambda) = exp\{-AM_p/[\lambda^4(115.6406 - 1.355/\lambda^2)]\}, \quad (6)$$

$$T_a(\lambda) = exp\left(-\beta \cdot \lambda^{-\alpha} \cdot AM_p\right), \quad (7)$$

$$T_w(\lambda) = exp\left[\frac{-0.2385 \cdot A_w(\lambda) \cdot w \cdot AM_p}{\left(1+20.07 \cdot A_w(\lambda) \cdot w \cdot AM_p\right)^{0.45}}\right], \quad (8)$$

$$T_o(\lambda) = exp[-A_o(\lambda) \cdot w_o \cdot m_o]\,, \quad (9)$$

$$m_o = \frac{35.0}{(1224.0\,cos^2(z)+1)^{0.5}}\,, \quad (10)$$

$$T_g(\lambda) = exp\left[\frac{-1.41 \cdot A_g(\lambda) \cdot AM_p}{\left(1+118.3 \cdot A_g(\lambda) \cdot AM_p\right)^{0.45}}\right]. \quad (11)$$

AM_p parameter in equations is the value of actual air mass provided by Whitaker and Newmiller in 1998 in the following form of Eq. (12) [19]:

$$AMp(t) = \frac{p}{p_0} \cdot [cos(z + 0.00094 \cdot (1{,}6389 - z)^{-1.253}]^{-1}. \quad (12)$$

More information about this can be accessed in Refs. 20 - 23 and in Refs. 24 - 27.

3. Atmospheric transparency parameter

3.1 *Beam clear sky index* (K_b)

The relation (proportion) between the value of the direct component beam reaching the Earth's surface and the value of intensity of the irradiation beam entering the upper atmosphere in the plane of horizon is the so-called beam clear sky index (K_b). It is the measure of the amount of beam irradiance available (proportion between beam irradiance and extra-terrestrial solar irradiance on a horizontal surface) [28–31]:

$$K_b(t) = \frac{G_{B,\,H}(t)}{G_{B,\,H0}(t)}\,. \quad (13)$$

The integration of Eq. (7) after λ produces a formula for irradiation transmittance as a function of two variables: β and AMp:

$$\int T_a(\lambda, \beta, AM_p)d\lambda = T_a(\beta, AM_p) \propto exp\left(-\beta \cdot AM_p\right). \quad (14)$$

The important aspect is that the value T_a transmittance of irradiation from extinction in aerosols is directly proportional to the factor $exp\left(-\beta \cdot AM_p\right)$. By analogy it can be determined for other transmittance functions, e.g., for Eq. (8), an expression for transmittance of irradiation connected with absorption by steam particles [Eq. (15)] can be obtained as the function w – content of steam and AM_p. This function is directly proportional to the factor - $exp\left[\frac{-0.2385 \cdot w \cdot AM_p}{\left(1+20.07 \cdot w \cdot AM_p\right)^{0.45}}\right]$:

$$\int T_w(\lambda, \beta, AM_p)d\lambda = T_w(w, AM_p) \propto exp\left[\frac{-0.2385 \cdot w \cdot AM_p}{\left(1+20.07 \cdot w \cdot AM_p\right)^{0.45}}\right]. \quad (15)$$

With the integration of Eq. (5) after λ and considering the definition of $K_b(t)$, the following is obtained:

$$\frac{G_{B,\,H}(t)}{G_{B,\,H0}(t)} = K_b(t) = A \cdot T_a(\lambda)T_w(\lambda)T_R(\lambda)T_0(\lambda)T_n(\lambda)T_g(\lambda), \quad (16)$$

where: A – proportionality constant.

Equation (16) determines that:
$K_b(t) \propto T_a(\lambda),\ T_w(\lambda),\ T_R(\lambda), \ldots$. In the case of transmittance connected with extinction in aerosol:

$$K_b(t) \propto T_a(t) = \frac{1}{exp\left(\beta(t) \cdot AM_p(t)\right)}\,. \quad (17)$$

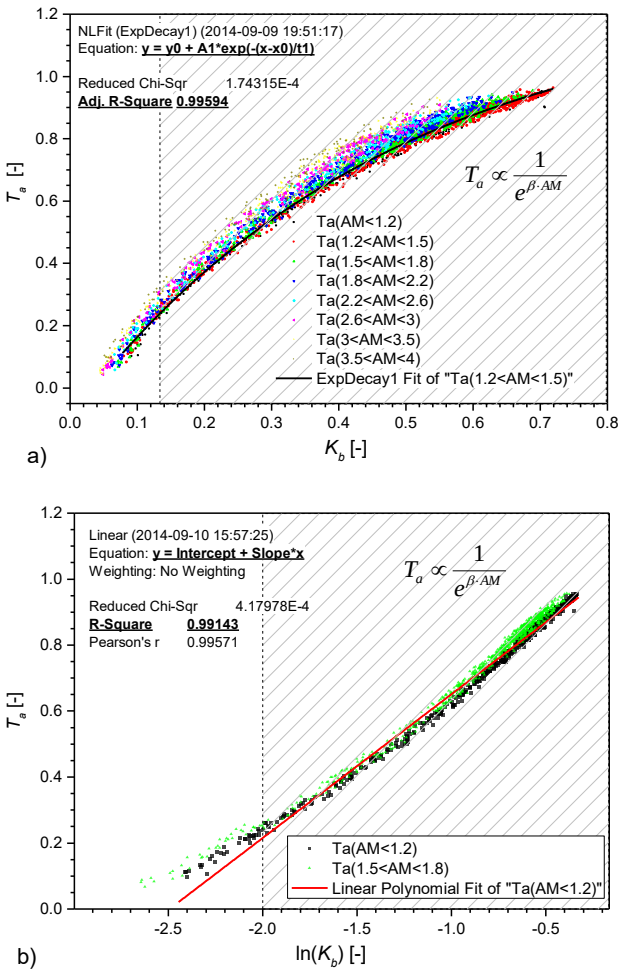

Fig. 1. a) Transmittance graph T_a connected with extinction in aerosols in the function K_b for the parametrically variable AM values, b) linear approximation of transmittance graph T_a in the function $ln(K_b)$ marking the linearity field of these relations. The graphs were prepared for two AM values: <1.2 and from the range of (1.5; 1.8).

By analogy, in the case of absorption of irradiation by steam:

$$K_b(t) \propto T_w(t) = exp\left[\frac{-0.2385 \cdot w(t) \cdot AM_p(t)}{\left(1+20.07 \cdot w(t) \cdot AM_p(t)\right)^{0.45}}\right]. \quad (18)$$

The exponential form of the factor from Eq. (17) indicates that the course of the diagram $ln(K_b(t))$, in the area of domination of the processes connected with aerosol extinction, should be linear [see Fig. 1b)].

$$ln\left(K_b(t)\right) \propto -\beta(t) \cdot AM_p(t). \quad (19)$$

In Fig. 1a) the course of irradiation transmittance was presented, at extinction in aerosol (T_a) described in Eq. (16) in the function of K_b for the parametrically variable value *AM*, whereas in Fig. 1b) linear approximation of transmittance graph T_a in the function $ln(K_b)$ for low values of *AM* (i.e., <1.2) and the area of linearity of these relations were marked as hatched. Additionally, the course of transmittance for mean *AM* values was projected, i.e., from the range of (1.5–1.8). As can be seen, distribution of these points in the graph is almost identical and demonstrates linearity of the transmittance T_a with logarithm of the index K_b for the value $ln(K_b)$>-2 with the coefficient R^2= 0.99143. In Fig. 2 a comparison of power yield was observed from a single junction amorphous silicon module, with reference to the power of irradiation G_{POA} falling on the surface of the tested model in the function of: a) transmittance – T_a, b) beam clear sky index – K_b. More information on the characteristics of the applied conversion function can be found in Ref. 6. In the studies, the value β – of Angstrom turbidity coefficient – was determined according to the procedures described in Refs. 5 and 32. Initial analysis proves that the obtained results are very similar.

In Fig. 3 the results' examples of the whole year of observation of a single junction amorphous silicon module operation were presented in the conditions of low and very low irradiance values. The studies were carried out for the typical *AM* values used in measurements of PV modules in outdoor conditions.

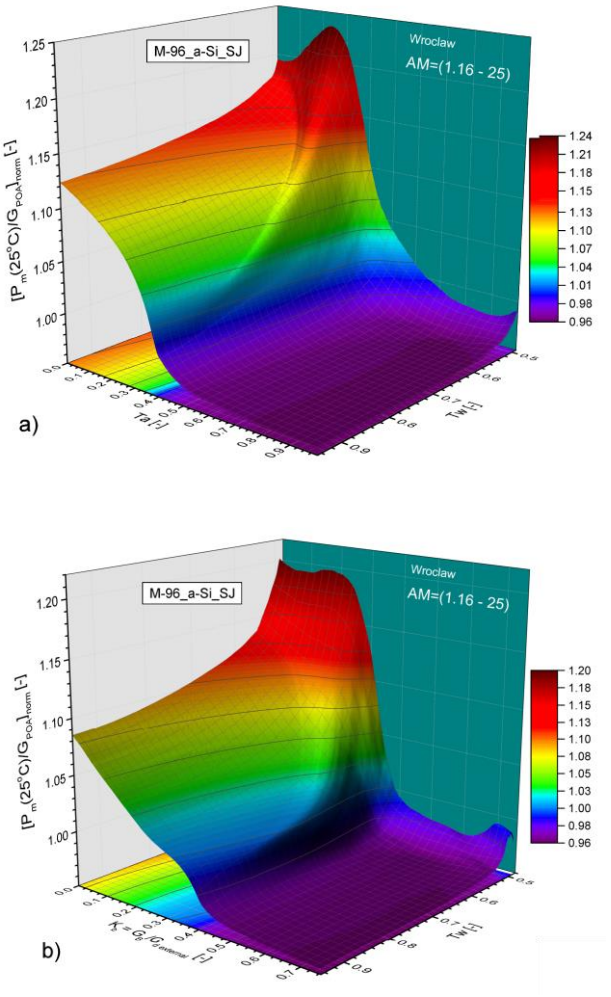

Fig. 3. Comparison of the study results of the obtained power of a single junction amorphous silicon module, in the function of: a) transmittance T_a connected with extinction in aerosols, b) K_b – beam clear sky index.

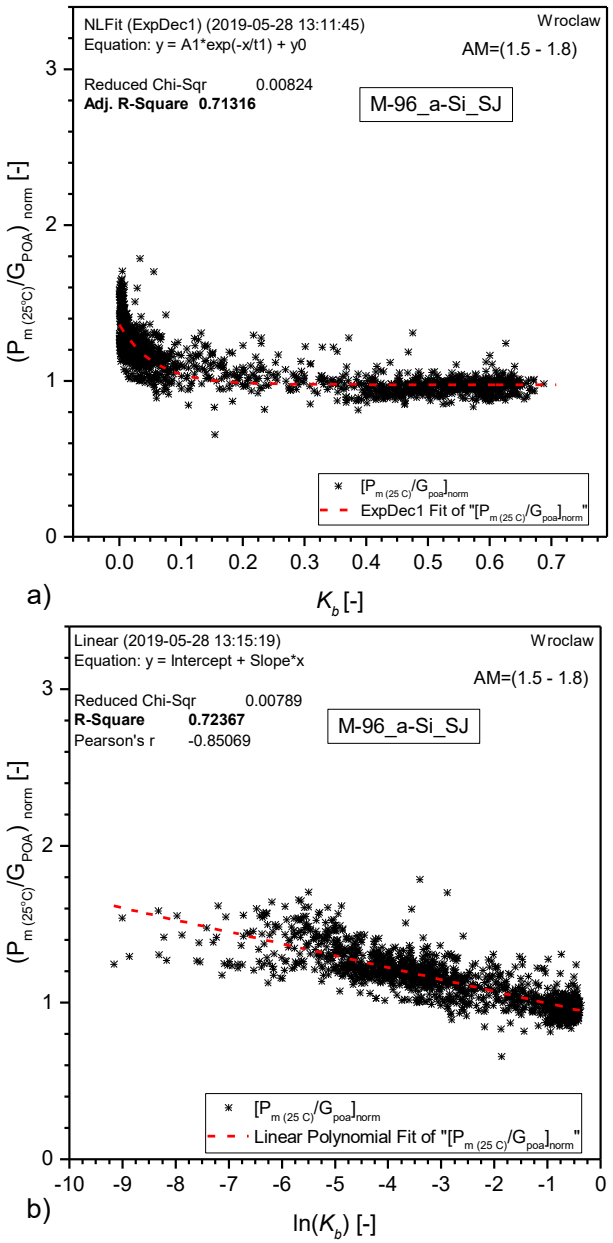

Fig. 2. Example of the operation analysis of a module made of amorphous silicon in the conditions of low and very low irradiance.

The value of AM <1.8 in the city of Wroclaw in summer months (i.e., from IV to IX) in the time range of (8 am – 4 pm) (Fig. 10). A comparison of figures a) and b) demonstrates that the use of $ln(K_b)$ results in the extension of the graph which reflects the range of low and very low irradiances, thus giving the possibility to thoroughly analyse a module conversion in the range of large attenuation of a direct irradiance component.

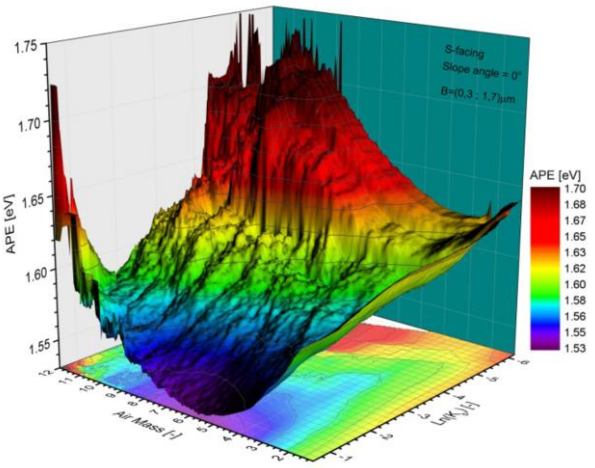

Fig. 4. Example of the application of the logarithm index K_b in the analysis of a distribution of the averaged values of photon energy (APE) in the function of a variable air mass value in the analysis, with the particular focus of the phenomena occurring in the area of low irradiance values. The studies were carried out for the city of Wroclaw.

In Fig. 4 the use of the logarithm beam clear sky index K_b for the analysis of the distribution of averaged values of photon energy (APE) in the function of variable air mass value is shown. All presented study results included in Figs. 1 - 4 were based on the data generated during all-year monitoring of the meteo and PV systems. As can be noticed, imaging of the results with the use of $ln(K_b)$ results in emphasising the result of the observation of phenomena occurring in the area of low and very low values of irradiance.

From the above we can conclude that: first, within the range of values $ln(K_b) \geq -2$, i.e., for $K_b \geq 0.135$, for the air mass value $AM \leq 4$ the occurrence with the coefficient $R^2 = 0.99143$ of the linear dependence between index $ln(K_b)$ and transmittance T_a was determined, which is connected with fogginess of the atmosphere [Fig. 1b)].

Secondly, the occurrence of a linear correlation between index $ln(K_b)$ and transmittance T_a allows for the influence of atmospheric fogginess in PV modules' operation to be observed (Fig. 2). The presented feature is even more significant, if a difficulty level of determination is considered of: K_b – beam clear sky index and coefficient β of Angstrom turbidity. The former can be determined in a simple way, contrary to the latter (β) [5,32].

Thirdly, the use of $ln(K_b)$ in testing modules supports observation of PV conversion capacity very well in the range of low and very low irradiance.

3.2 *Clear sky index/content of the diffused component*

The relation between the global value ($G_{0,H}$) of the intensity of irradiance falling on the Earth's surface, entering the upper atmosphere in the plane of horizon, is the measure of atmosphere clarity and is described by the clear sky index1[1] k_{Tm}. The index is directly converted on the content of the diffused component in global irradiance falling on the horizon plane, defined in literature as the index of diffused component content ($k_{s/o}$) [Fig. 5a)] [33-36] and in Ref. 37:

$$k_{Tm}(t) = \frac{G_{0,H}(t)}{\frac{G_{d\ external}}{AM_p(t)}}, \tag{20}$$

$$k_{\frac{s}{o}}(t) = \frac{G_{S,H}(t)}{G_{0,H}(t)}. \tag{21}$$

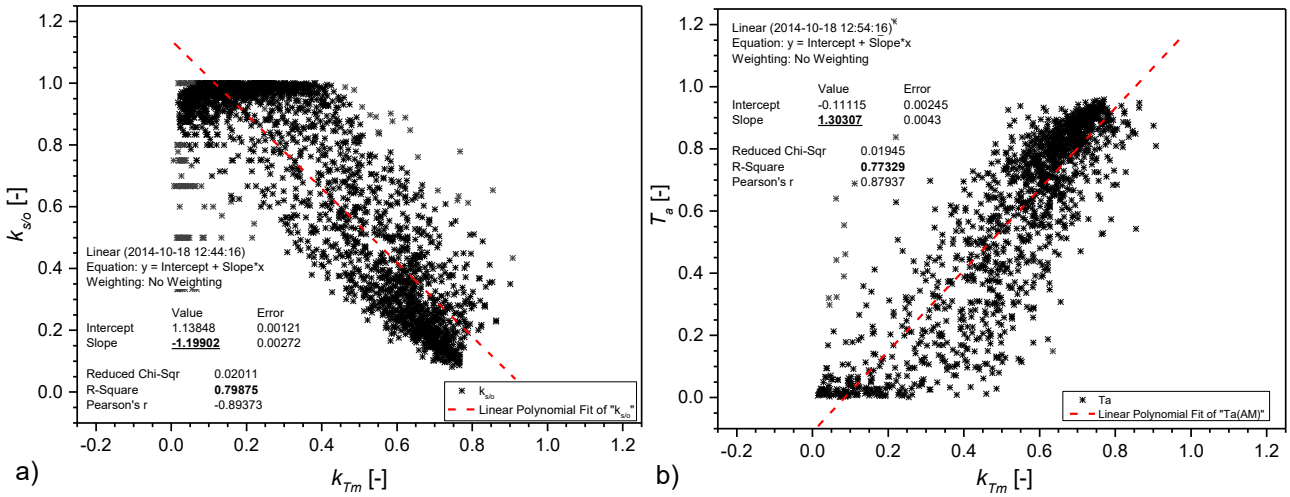

Fig. 5. Influence of the clear sky index k_{Tm} on a) atmosphere clearness index $k_{s/o}$, b) transmittance connected with extinction in aerosols. Imaging of the results of all-year data monitoring from the local meteo station in Wroclaw.

[1] * It is also referred to as: atmosphere transparency index or clear sky index.

Similarly to the instantaneous values, daily, monthly and yearly values of these indexes can be determined, for example:

– daily value of clear atmosphere index , as:

$$k_{Tm_{day}} = \frac{E_{0,H}(0)}{E_C(0)}, \tag{22}$$

– daily value of the content of the diffused component of irradiance index, as:

$$k_{s/o\_day} = \frac{E_{S,H}(0)}{E_{0,H}(0)}. \tag{23}$$

In Fig. 5a) a mutual correlation of the diffused component index $k_{s/o}$ and the clear sky index k_{Tm} is presented, whereas in Fig. 5b) a correlation of the transmittance index T_a with the clear sky index k_{Tm} is shown. Comparison of distribution (concentration) of measurement points in the graphs: Fig. 5b) and Fig. 1 (for which the value of R^2 was of 0.99143), the results show that there is no strong direct correlation between transmittance index T_a and clear sky index k_{Tm}.

Figures 6a) - 6i) present examples of daily values of clear atmosphere indexes and diffused component content in the global value of irradiance during days with various values of daily irradiance. The presented daily values of indexes k_{Tm} and $k_{s/o}$ were determined according to Eq. (22) and Eq. (23). In Fig. 7 the connection between the beam clear sky index K_b and the diffused component content index $k_{s/o}$ was presented, where in Fig. 7a) consolidation of points for six air mass value ranges, whereas in Fig. 7b) (blue field) differences in approximation curves: filtered low values of *AM*, i.e., *AM*=(1.2;1.5), marked in the graph

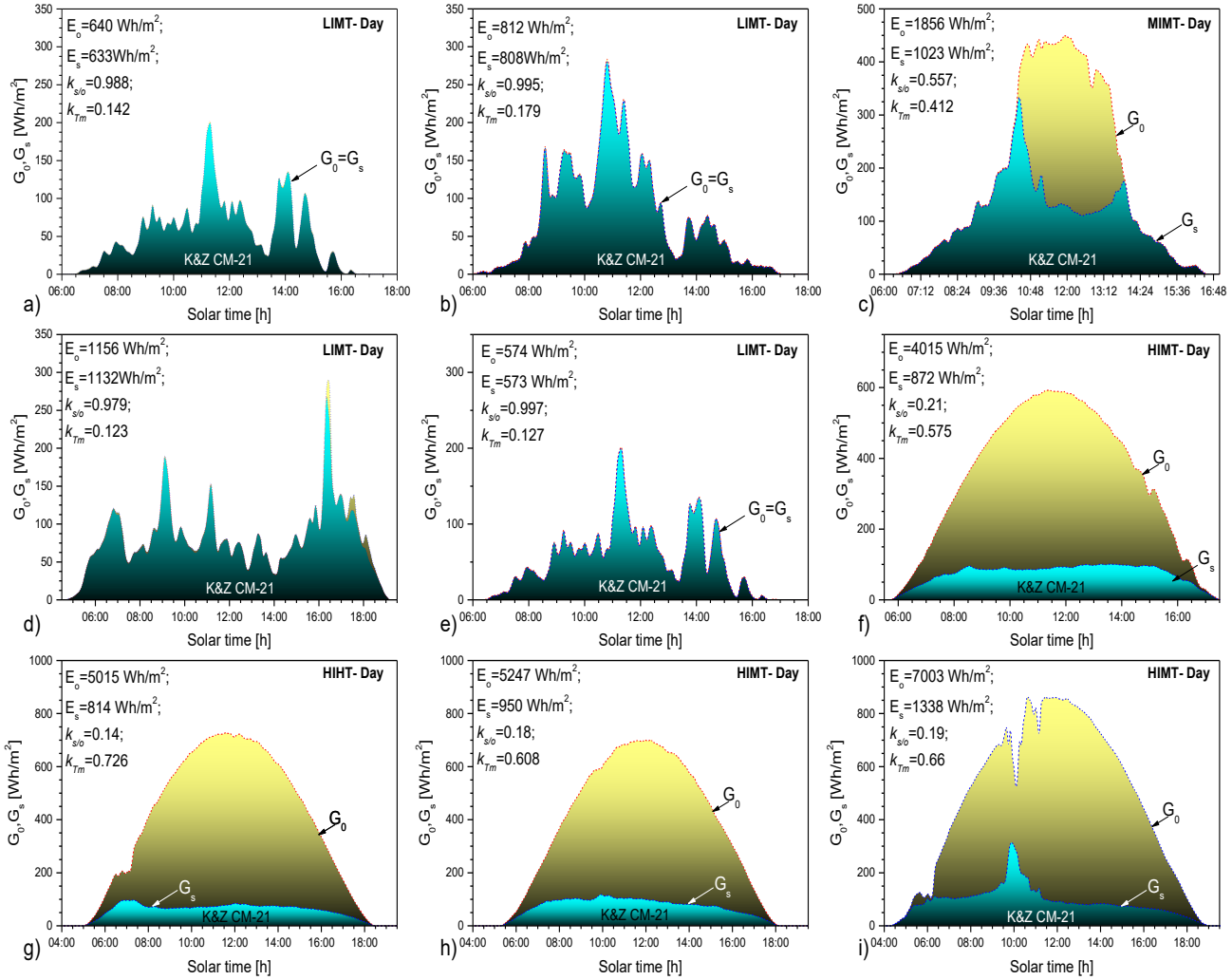

Fig. 6. Example of the summary index of global irradiance and the related clear atmosphere index, as well as diffused component content during days[1] with various irradiance values. The studies were carried out for the city of Krakow.

[1] Type of day: HIHT (high irradiance, high temperature), MIHT (medium irradiance, high temperature), HILT (high irradiance, low temperature), LILT (low irradiance, low temperature), MIMT (medium irradiance, medium temperature).

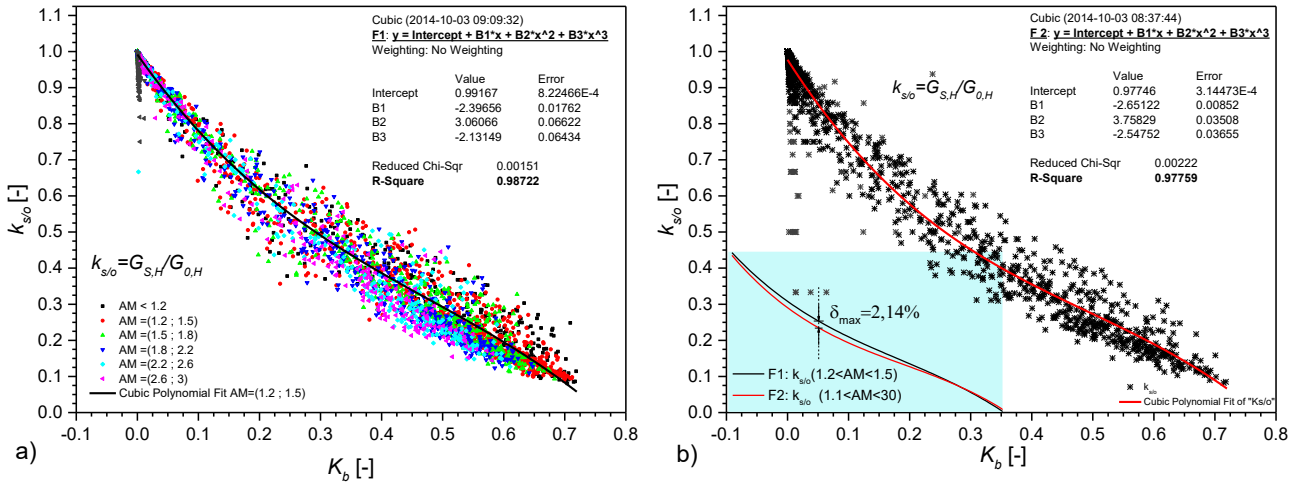

Fig. 7. Connection between the beam clear sky index (K_b) and the diffused component content index ($k_{s/o}$). Imaging for: a) parametrically variable air mass from the range of 1.2–3, and b) influence of air mass on the approximation function. Studies were carried out for the city of Krakow.

as F1 with the coefficient R^2=0.98722, and a full range of occurrence, i.e., from the range of (1.1; 30) marked in the graph as F2 with the coefficient R^2=0.97759. As can be seen, the maximum difference error between those curves does not exceed δ_{max}=2.14 %. Obtaining such high determination coefficients for approximation curves F1 and F2 and their high convergence in a wide range of air mass values demonstrates a high level of correlation between the beam clear sky index K_b and the diffused component content index $k_{s/o}$.

The presented indexes: atmosphere transparency index or diffused component content are physically connected not only with the irradiance path through the Earth's atmosphere, which depends on the *AM* value, but also on the chemical composition and cloudiness of the atmosphere. Liu and Jordan [38] demonstrated that regardless of geographical latitude, the global value of irradiance intensity reaching the Earth's surface depends directly on this parameter.

That is why the index can correctly describe irradiance conditions of individual locations. It can also provide information on the average photon energy in the spectrum and on the very structure of the irradiance spectrum. For example, the diffused component content index $k_{s/o}$ directly describes the cloudiness level. It also provides information on the average photon energy (see Fig. 8).

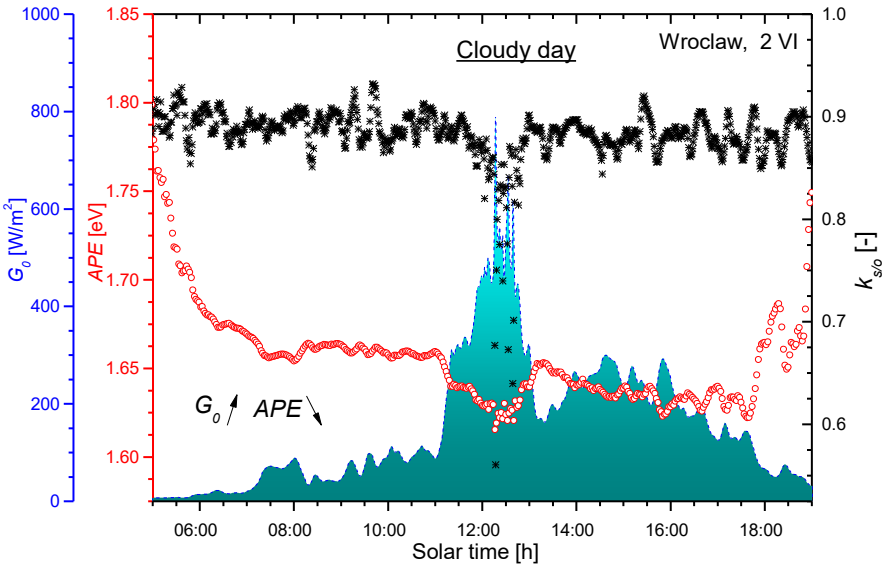

Fig. 8. Diffused component content index; average photon energy of irradiance and global intensity of irradiance on a cloudy day.

3.3 *The use of indexes in the analysis of solar energy resources for PV*

The discussed indexes are very useful in preparing correct characteristics of the selected locations in order to select the optimal modules for the locally prevailing climate conditions. The annual distribution of averaged daily values, together with the distribution of averaged daily insolation values characterize the potential resources of solar energy for PV purposes.

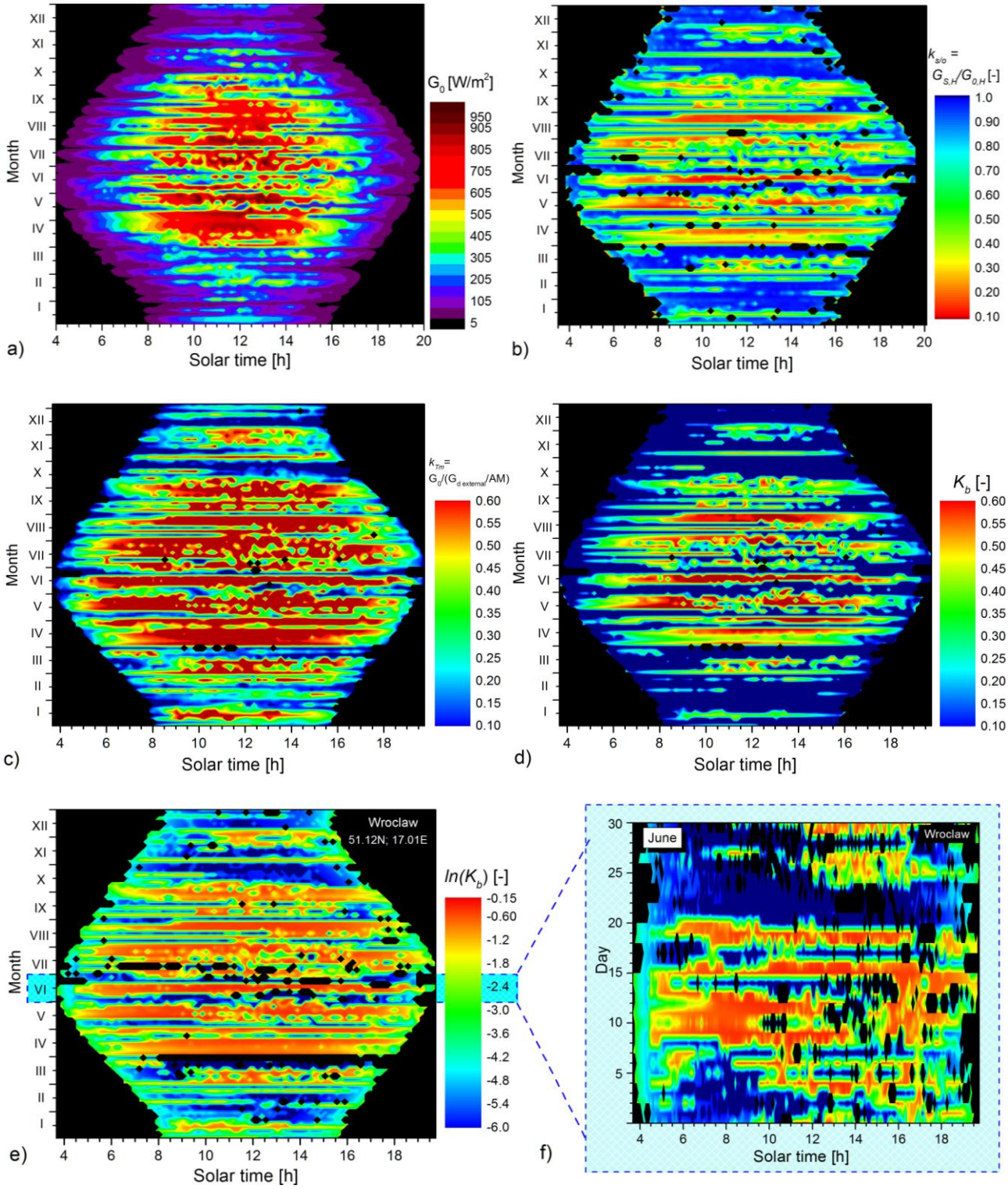

Fig. 9. Distribution of instantaneous values: a) solar irradiance intensities $G_{0,H}$, b) diffused component content index $k_{s/o}$, c) sky clearness index k_{Tm}, d) beam clear sky index K_b, and e) logarithm of beam clear sky index $ln(K_b)$ – occurring in the laboratory SolarLab in Wroclaw during PV modules testing. The enlarged field f) presents distribution of attenuation of direct component $ln(K_b)$ in June in Wrocław.

In Fig. 9a) a distribution of irradiance falling on the plane of horizon in the location of tested modules is presented. It should be emphasised that the changes of both irradiance rate value and the Sun activity times occur in a very wide range. The obtained data is used in determining the so-called area insolation, i.e., determining an average number of hours of solar activity in each month, sufficient[2] for a PV operation.

Figures 9e) and 9f) show the annual and monthly distribution of the logarithm beam clear sky index K_b. As shown, the index allows for a detailed analysis to be carried out in the areas of low and very low insolation. This is dedicated for analyses of the PV modules' conversion capacity in conditions of low and very low insolation.

3.4 *Relations between atmospheric transparency indexes/parameters and spectral distribution of irradiance*

a) Analyses in the function of instantaneous values

In order to present clear Krakow images of the data from all-year observations, data was segregated into nine subgroups (Fig. 10).

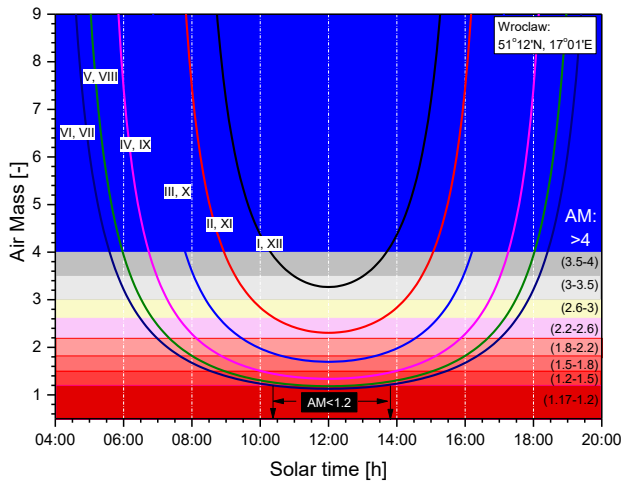

Fig. 10. Correlations of the analysed *AM* values ranges with the day, time and season of the year for the city of Wroclaw.

The subgroup, for which *AM*<1.2, includes the data from the south, with the lowest *AM* values – considering time, it offers the best measurement conditions for cells and measuring equipment calibration. The second group, i.e., for the measurements carried out at *AM*=(1.2–1.5), includes the measurement data from a typical time period, during which cells and PV modules' measurements are taken in outdoor conditions. The obtained data is always used to translate the results into STC conditions. The third area, *AM*=(1.5–1.8), is still suitable for taking measurements of PV modules. The areas from the fourth to the eighth – time areas are used in testing photovoltaic operation/conversion of PV modules and cells in natural conditions. The area nine, i.e., for which the value of *AM*>4, is the time area used for analysing PV modules' conversion in operating conditions, during sunrise/sunset, i.e., in the conditions with a very high content of the diffused component of irradiation. For example, in the location where the studies were carried out, i.e., AGH Krakow and SolarLab Wroclaw, testing of PV modules in the conditions of air mass *AM*>8 refers in reality to testing only with the diffused component in which the spectrum is strongly modelled by long-wave absorption component phenomena (mainly by steam) and scattering: by the particles with a diameter of less than 0.1 of the light wavelength, e.g., N_2 and O_2 molecules described by Rayleigh's theory [10] and by particles suspended in the atmosphere with a diameter larger than 0.1 of the light wavelength, referred to as the atmosphere turbidity $\tau_a(\lambda)$, described by Mie's theory [39-42]. The whole phenomenon is emphasised by the total path of a sunbeam of the diffused component going through the Earth's atmosphere. The phenomenon of beam diffusion by clouds, rain, snow and hail reduces intensity of irradiance on the Earth's surface, according to the model prepared by Mie [43]. In most cases, influence of this phenomenon on the value of irradiance intensity and its spectral distribution can be described by determining the function of spectrum modification for a cloudy day, depending on three variables: wavelength, value of air mass index and content of a diffused component in the global irradiance value [44].

Due to the large number of charts presented in the article and the need to maintain their readability, other examples are included in the Attachment.

b) Analysis of daily energy values

Figures 11 - 13 present the influence of daily values of the respective index: diffused component (k_{s/o_day}), beam clear sky (K_{b_day}), logarithm of beam clear sky index [$ln(K_{b\_day})$] – irradiance on a) – e) averaged daily content of useful fractions UF_{day}, f) average daily value of *APE* – of irradiation falling on the plane of horizon. The presented results were obtained with reference to band B=(0.3; 1.7) μm of spectroradiometer. The daily values of indexes used in the analyses were determined according to: Eq. (22) and Eq. (23). The daily value of the beam clear sky index K_{b_day} was determined according to Eq. (24):

$$K_{b\_day} = \frac{E_{B,H}(0)}{E_G(0)}. \tag{24}$$

The obtained results confirm the observed tendencies in changes of the content of *UF* in the function of daily values of clear atmosphere parameters, i.e., daily values of clear sky index – k_{Tm_day}, diffused component content index – k_{s/o_day}, or beam clear sky index – K_{b_day}. Similarly, as in the case of analyses with the use of instantaneous values (k_{Tm}, $k_{s/o}$, or K_b), in the analyses with the use of energy values very good characteristics of $ln(K_b)$ can be noticed in the studies of the areas with low and very low insolation.

[2] Typical photovoltaic inverter has a characteristic threshold of DC input power connected to the area of this work at maximum efficiency. For properly designed PV system that threshold inverter DC input power corresponds to the value of solar radiation of ≈ 200 W/m^2. Then, a typical efficiency of the inverter is already above 95% of its maximum efficiency.

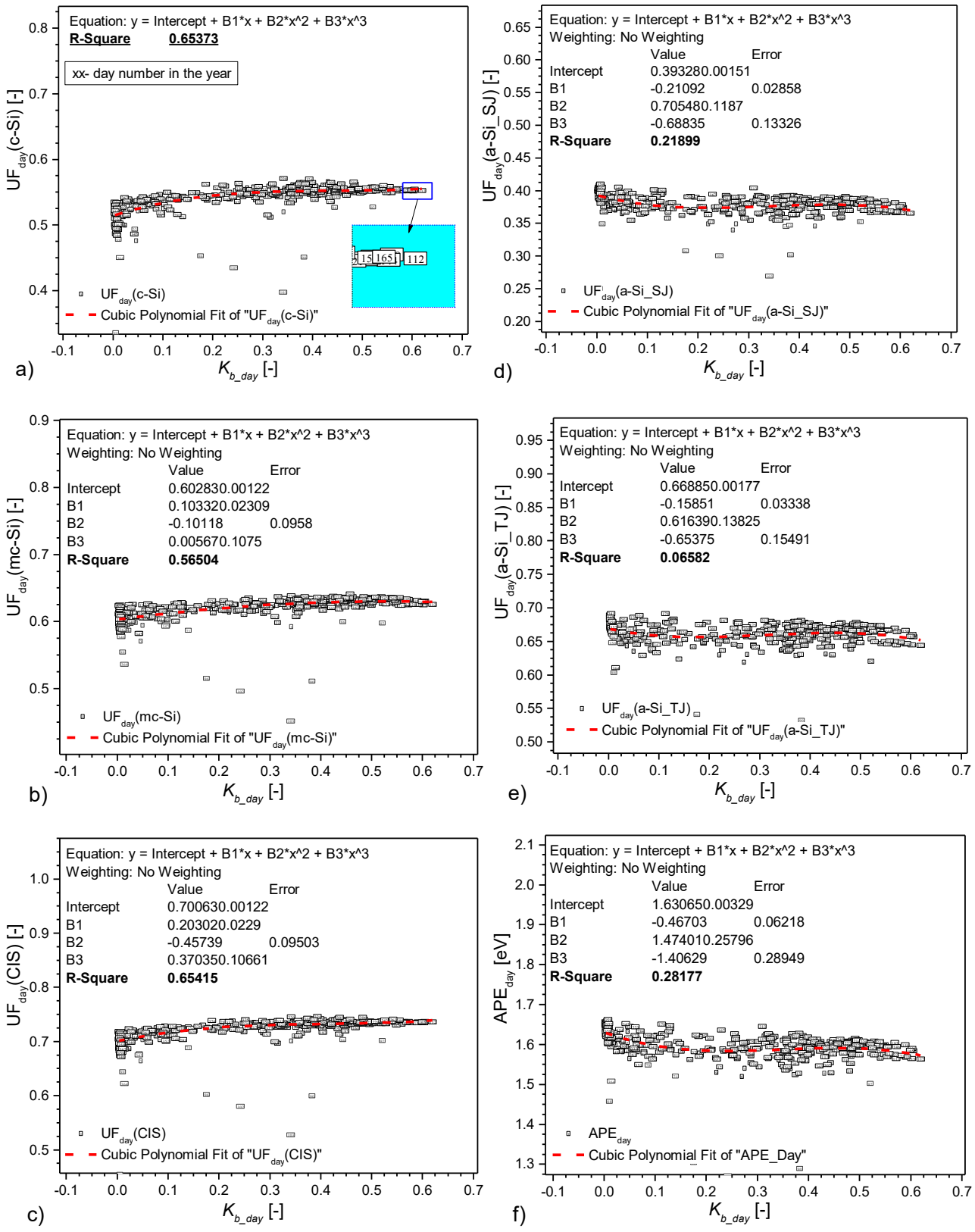

Fig. 12. Influence of daily value of the beam clear sky index (K_{b_day}) of irradiance on: a) – e) averaged daily content of useful fractions UF_{day}, f) average daily value of *APE* – of irradiance falling on the plane of horizon. The presented results were obtained with reference to band B=(0.3;1.7) μm of the measuring spectroradiometer. The studies were carried out for the city of Krakow (POA Modules: S-facing, Slope 0°).

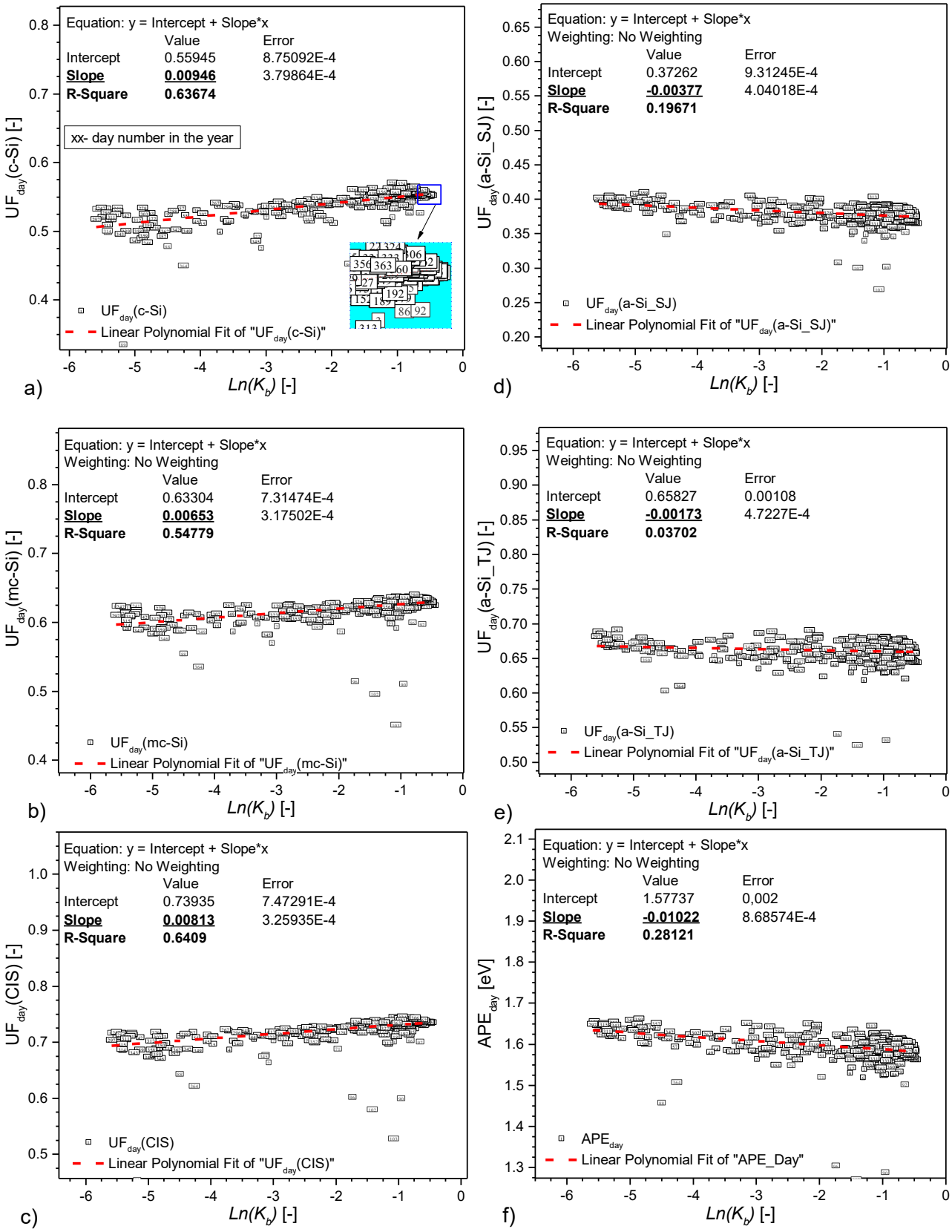

Fig. 13. Influence of daily value of the beam clear sky index logarithm $ln(K_{b\_day})$ of irradiance on: a–e) averaged daily content of useful fractions UF_{day}, f) average daily value of *APE* – of irradiance falling on the plane of horizon. The presented results were obtained with reference to band B=(0.3;1.7) μm of the measuring spectroradiometer. The studies were carried out for the city of Krakow (POA Modules: S-facing, Slope 0°).

4. CONCLUSIONS

The following conclusions can be drawn from the research carried out:

The use of atmosphere transparency parameters, such as: atmosphere transparency index k_{Tm}, diffused component content index $k_{s/o}$, beam clear sky index K_b is a cheap and very practical method of testing module conversion capacity in actual operating conditions.

The occurrence of the linear correlation between index $ln(K_b)$ (logarithm of beam clear sky index) and transmittance T_a, allows for the influence of atmospheric fogginess on a PV module operation to be observed. The presented feature is even more significant if one considers the difficulty level of determination of K_b – beam clear sky index and coefficient β of Angstrom turbidity. The first can be determined in a very simple way, contrary to the second β.

The use of $ln(K_b)$ in testing modules supports observation of a PV conversion capacity very well in the range of low and very low irradiance.

Making long-term studies of a PV module conversion capacity in outdoor conditions provides a full picture of usefulness in specific climate conditions, characteristic for higher geographical latitudes inparticular. In this context, the use of transparency indexes in the above-mentioned studies becomes indispensable.

The main problem with measurements using sunlight is its large spectral changeability which means that the measurement conditions using natural sunlight restrict its possibilities. The measurements can be carried out only in appropriate conditions. In natural conditions, even for the same day, spectral distribution of solar radiation of the same *AM* from before and after noon is different which results in different measurement outputs for the same PV cells and modules. In this context, due to the occurrence of a strong connection between atmosphere transparency parameter and spectral parameters which characterize irradiance, such as *APE* or *UF* (see chapter 3), determined in a simple and cheap way atmosphere transparency parameters are very useful in characterising atmospheric conditions during the studies.

The data obtained during long-term actinometric measurements, including the above-mentioned parameters, precisely characterise the structure of solar energy resources of a region for photovoltaic purposes. The maps of their annual distribution in the dedicated climate zones should be used as the main input parameter in optimising newly created cells and modules dedicated to operation in such geographical and climate conditions. They provide a full picture of the modules' usefulness in specific climate conditions characteristic for the areas at higher geographical latitudes. In this context, the use of clearness index in the above-mentioned studies becomes indispensable.

In this context, due to the occurrence of a strong connection between the atmosphere transparency parameter and spectral parameters, such as *APE* or *UF* (see chapter 3), the obtained results can be skilfully used (i.e., with proper understanding) with clearness indexes which in practice may totally replace the need to carry out studies using spectral parameters of *irradiance* which require the application of very expensive measuring equipment, i.e., their analysis should lead to the same conclusions which are obtained as a result of research using spectral parameters.

The authors hope that the above publication shall contribute to popularising the presented research methods as a cheap and effective method of estimating usability of modules to operate outdoors. This will allow for the research to be intensified on the optimisation of newly created cells and modules to the conditions reflecting actual climatic conditions in specified geographical regions.

Acknowledgements:

The authors wish to thank doctor engineer Tadeusz Żdanowicz from Wroclaw Technical University and Janusz Teneta, PhD from AGH Krakow for disclosing their measurement data to carry out the above analyses, their help and assistance in implementing the study and editing this article.

References:

[1] Rodziewicz, T., Teneta, J., Zaremba, A. & Wacławek, M. Analysis of Solar Energy Resources in Southern Poland for Photovoltaic Applications. *Ecol. Chem. Eng. S* **20**, 177–198 (2013). https://doi.org/10.2478/eces-2013-0014

[2] Chojnacki J., Teneta J., Wieckowski L. Development of PV systems and research studies on photovoltaics at the AGH University of Science and Technology in Krakow, 22nd European Photovoltaic Solar Energy Conference, Conference Proceedings, 3049–3052 (2007). https://www.eupvsec-proceedings.com/

[3] Zdanowicz, T., Prorok, M., Kolodenny, W., Roguszczak, H. Outdoor data acquisition system with advanced database for PV modules characterization,3rd WCPEC (2003), http://www.pvsc-proceedings.org/.

[4] Zdanowicz, T., Roguszczak, H. Automated outdoor data acquisition system for prolonged testing of PV modules, Proc 13th EC PV Solar Energy Conference 2322 (1995). https://www.eupvsec-proceedings.com/.

[5] Rodziewicz, T. & Rajfur, M. Numerical procedures and their practical application in PV modules analyses. Part I: air mass. *Opto-Electron. Rev*. **27**, 39–57 (2019). https://doi.org/10.1016/j.opelre.2019.02.002

[6] Rodziewicz, T. & Rajfur, M. Numerical procedures and their practical application in PV modules' analyses. Part II: Useful fractions and APE. *Opto-Electron. Rev.* **27**, 149–160 (2019). https://doi.org/10.1016/j.opelre.2019.05.004.

[7] Hu, C., & Richard M. *White. Solar Cells: From Basics to Advanced Systems*. (New York: McGraw-Hill, 1983). https://www.worldcat.org/title/solar-cells-from-basics-to-advanced-systems/oclc/924887007.

[8] Spencer, J.W. Fourier Series Representation of the Position of the *Sun. Search* **2,** 162-172 (1971)

[9] Myers, J. D. Solar applications in industry and commerce. (Prentice Hall PTR, 1984)

[10] Tendeku, F. Retrieval of Atmospheric Turbidity Coefficient and Water Column Density from Solar Irradiance Data, *Proc. Arkansas Acad. Sci. **49,** 177-180 (1995).* https://scholarworks.uark.edu/jaas/vol49/iss1/38/

[11] Tendeku, F. A method for determining atmospheric aerosol optical depth using solar transmission measurements. *Proc. Arkansas Acad. Sci.* **48**, 192-195 (1994). http://scholarworks.uark.edu/jaas/vol48/iss1/39

[12] Penndorf, R. Tables of the refractive index for standard air and the Raleigh scattering coefficient for the spectral region between 0.2 and 20.0 and their application to atmospheric optics. *J. Opt. Soc. Am*. **47**, 176-182 (1957). https://doi.org/10.1364/JOSA.47.000176

[13] Kneizys, F.X., Shettle, E.P *et al*. Atmospheric Transmittance/ Radiance: Computer code LOW TRAN5. *Tech. Rep. AFGL-TR-80-*

0067. US Air Force Geophysics Laboratory (Bedford, Massachusetts, 1980).

[14] Kasten, F., Young A.T. Revised optical air mass tables and approximation formula. *Applied Optics*. **28**, 4735-4738 (1989) https://doi.org/10.1364/AO.28.004735

[15] F. Kasten, The Linke turbidity factor based on improved values of the integral Rayleigh optical thickness, *Solar Energy* **56**, 239– 244 (1996). https://doi.org/10.1016/0038-092X(95)00114-7.

[16] B. Leckner, The Spectral distribution of solar radiation at the earth's surface - elements of a model. *Solar Energy* **20**, 143-150 (1978). https://doi.org/10.1016/0038-092X(78)90187-1

[17] Bird, R.E. A simple spectral model for direct normal and diffuse horizontal irradiance. *Solar Energy*. **32**, 461-471 (1984). https://doi.org/10.1016/0038-092X(84)90260-3

[18] Vigroux, E. Contribution a l'etude experimentale de l'absorption de l'ozone. *Annales de Phys.* **8**, 709-762 (1953). https://doi.org/10.1051/anphys/195312080709

[19] Whitaker, C., Newmiller, J. Photovoltaic Module Energy Rating Procedure. Final Subcontract Report, *New miller Endecon Engineering San Ramon* (California, 1998), NREL contract No. DE-AC36-83CH10093.

[20] Moskalenko, N. The spectral transmission function in the bands of water vapor, O_3, N_2O, and N_2 atmospheric components. *Izv. Acad. Sci. USSR Atmos. Oceanic Phys.* **5**, 678-685 (1969).

[21] Koepke, P., Quenzel, H. Water vapor: Spectral transmission at wavelengths between 0.7 μm and 1 μm. *Appl. Opt.* 17, 2114-2118 (1978). https://doi.org/10.1364/AO.17.002114.

[22] Gueymard, Ch. Parametrizied transmittance model for direct beam and circumsolar spectral irradiance. *Solar Energy* 71, 325-346 (2001), https://doi.org/10.1016/S0038-092X(01)00054-8.

[23] Feussner, K., Dubois, P., Trübungsfactor, precipitable water. *Staub. Gerlands Beitr. Geophys.* **27**, 132-175 (1930).

[24] Grenier, J.C., Casiniere, De La A. & Cabot, T. A spectral model of Linke's turbidity factor and its experimental implications. *Solar Energy* **52**, 303-313 (1994), https://doi.org/10.1016/0038-092X(94)90137-6.

[25] Gueymard, C., Vignola, F. Determination of atmospheric turbidity from the diffuse-beam broad-band irradiance ratio. *Solar Energy*. 63, 135–146 (1998), https://doi.org/10.1016/S0038-092X(98)00065-6.

[26] Heuklon, Van T.K. Estimating atmospheric ozone for solar radiation models, *Solar Energy*, 22, 63–68 (1979), https://doi.org/10.1016/0038-092X(79)90060-4.

[27] Viswanadham, Y. The relationship between Total Precipitable Water and Surface Dew Point, *J. Appl. Meteo.* **20**, 3–8 (1981), https://www.jstor.org/stable/26179402.

[28] Hofierka, J., Súri, M. The solar radiation model for Open source GIS: implementation and applications. *Proceedings of the Open source GIS - GRASS users conference* (2002), http://www.ing.unitn.it/~grass/conferences/GRASS2002/proceedings/proceedings/pdfs/Hofierka_Jaroslav.pdf

[29] Šúri, M., Dunlop, E.D. & Jones, A.R. GIS-based inventory of the potential photovoltaic output in Central and Eastern Europe. *PV in Europe. From PV Technology to Energy Solutions, Conference and Exhibition* (2002) http://citeseerx.ist.psu.edu/viewdoc/download?doi=10.1.1.572.9254&rep=rep1&type=pdf

[30] Ineichen, P., Perez, R. A new air mass independent formulation for the Linke turbidity coefficient. *Solar Energy* **73**, 151-157 (2002), https://doi.org/10.1016/S0038-092X(02)00045-2.

[31] Wright, J., Perez, R. & Michalsky, J.J. Luminous efficacy of direct irradiance: variations with insolation and moisture conditions, *Solar Energy* **42**, 387–394 (1989), https://doi.org/10.1016/0038-092X(89)90057-1.

[32] Gueymard, C.A. Turbidity Determination from Broadband Irradiance Measurements - A Detailed Multicoefficient Approach. *J. Appl. Meteorol.* 37, 414-435 (1998), https://doi.org/10.1175/1520-0450(1998)037%3C0414:TDFBIM%3E2.0.CO;2.

[33] Perez, R., Seals, R., Ineichen, P., Steward, R. & Menicucci, D. A new simplified version of the Perez diffuse irradiance model for tilted surfaces. *Solar Energy* 39, 221-231 (1987), https://doi.org/10.1016/S0038-092X(87)80031-2.

[34] Ineichen, P., Perez, R. Derivation of Cloud Index from Geostationary Satellites and Application to the Production of Solar Irradiance and Daylight IL luminance Data, *Theor. Appl. Climatol*. 64, 119-130 (1999), https://doi.org/10.1007/s007040050116

[35] Perez, R., Ineichen, P., Seals, R. & Zelenka, A. Making full use of the clearness index for parameterizing hourly insolation conditions. *Solar Energy* 45, 111-114 (1990). https://doi.org/10.1016/0038-092X(90)90036-C.

[36] Batlles, F.J., Olmo, F.J., Tovar, J. & Alados-Arboledas, L. Comparison of cloudless sky parameterisation of solar irradiance at various Spanish midlatitude Locations, *Theor. Appl. Climatol*. **66**, 81–93 (2000), https://doi.org/10.1007/s007040070034

[37] McKenney, D.W., Mackey, B.G. & Zavitz, B.L. Calibration and sensitivity analysis of a spatially-distributed solar radiation model. Inter. *J. Geograph. Inform. Sci*. **13**, 49-65 (1999), https://cfs.nrcan.gc.ca/publications?id=9783.

[38] Liu, B.Y.H. & Jordan, R.C. The interrelationship and characteristic distribution of direct, diffuse and total solar radiation, *Solar Energy* **4**, 1-19 (1960), https://doi.org/10.1016/0038-092X(60)90062-1

[39] Mie, G. Contributions to the optics of turbid media, especially colloidal metal suspensions, *Ann. Phys.* **25**, 377- 445 (1908), https://doi.org/10.1002/andp.19083300302.

[40] Born, M. & Wolf, E. *Principles of optics*. (Pergamon Press, Oxford 1970) https://archive.org/details/PrinciplesOfOptics.

[41] Stratton J.A. *Electromagnetic theory*. (McGraw-Hill Book Company, Inc., New York 1941), https://archive.org/details/electromagnetict031016mbp/page/n6.

[42] Bohren, C.F. & Huffman D.R. *Absorption and scattering of light by small particles*. (John Wiley & Sons, Inc., New York 1983). https://www.wiley.com/en-us/Absorption+and+Scattering+of+Light+by+Small+Particles-p-9780471293408

[43] Bazhan, W. Rozpraszanie światła na pojedynczych mikrocząstkach [Light scattering on individual microparticles], Doctoral thesis, Institute of Physics, Polish Academy of Sciences, (2004), http://www.ifpan.edu.pl/ON-2/on22/thesis.html [in Polish]

[44] Bird, R.E. & Riordan, C. Simple Solar Spectral Model for Direct and Diffuse Irradiance on Horizontal and Tilted Planets and the Earth's Surface for Cloudless Atmospheres, *J. Climate Appl. Meteorol.* 25, 87-97 (1986), https://doi.org/10.1175/1520-0450(1986)025<0087:SSSMFD>2.0.CO;2

Attachment

The presented figures (Figs. A1 - A14) are detailed descriptions of the local research environment in which long-term studies of PV modules have been carried out.

Figures A1a) – A1e) present the observed influence of air mass value (*AM*) on the content of useful fractions (*UF*) and the level of averaged photon energy values [Fig. A1. f)] – in the spectrum of irradiance falling on the plane of horizon; whereas Figures A2a) – A2e) present the observed influence of the averaged photon energy (*APE*) on the content of useful fractions (*UF*) in irradiance spectrum. The presented results were obtained with reference to band B=(0.3; 1.7) μm of the measuring spectroradiometer. The description of methodology of determining *UF* and *APE* is included in Ref. 1 and Ref. 6.

The consecutive figures present the determined distributions of useful fractions for the absorbers used in PV modules, in the function of: clear sky index value k_{Tm} – Figs. A3 - A6; diffused component index value $k_{s/o}$ – Figs. A7 - A10 and $ln(K_b)$ – Figs. A11 - A14.

Attachment - Supplementary materials

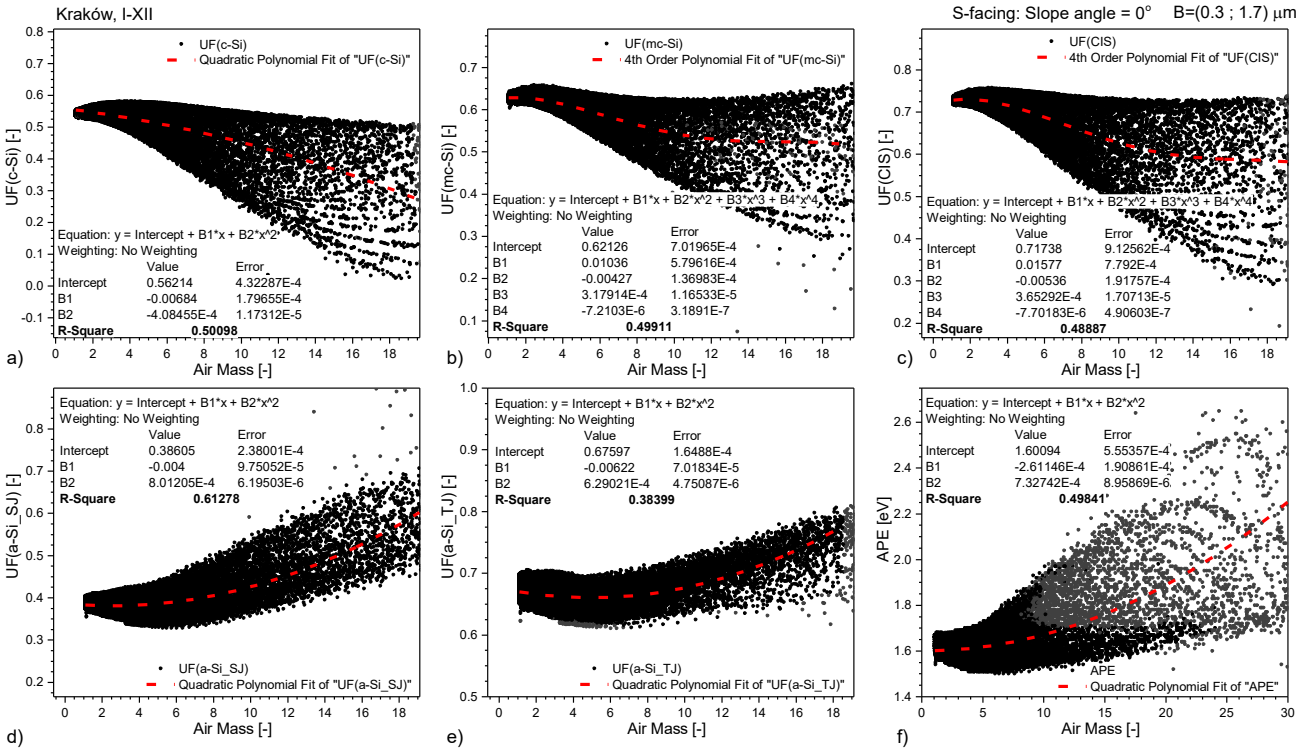

Fig. A1. The value of *AM* on: a–e) content of *UF*, f) value of *APE* – of irradiance falling on the horizontal plane. The presented results were obtained with reference to band *B*=(0.3; 1.7) µm of the measuring spectroradiometer.

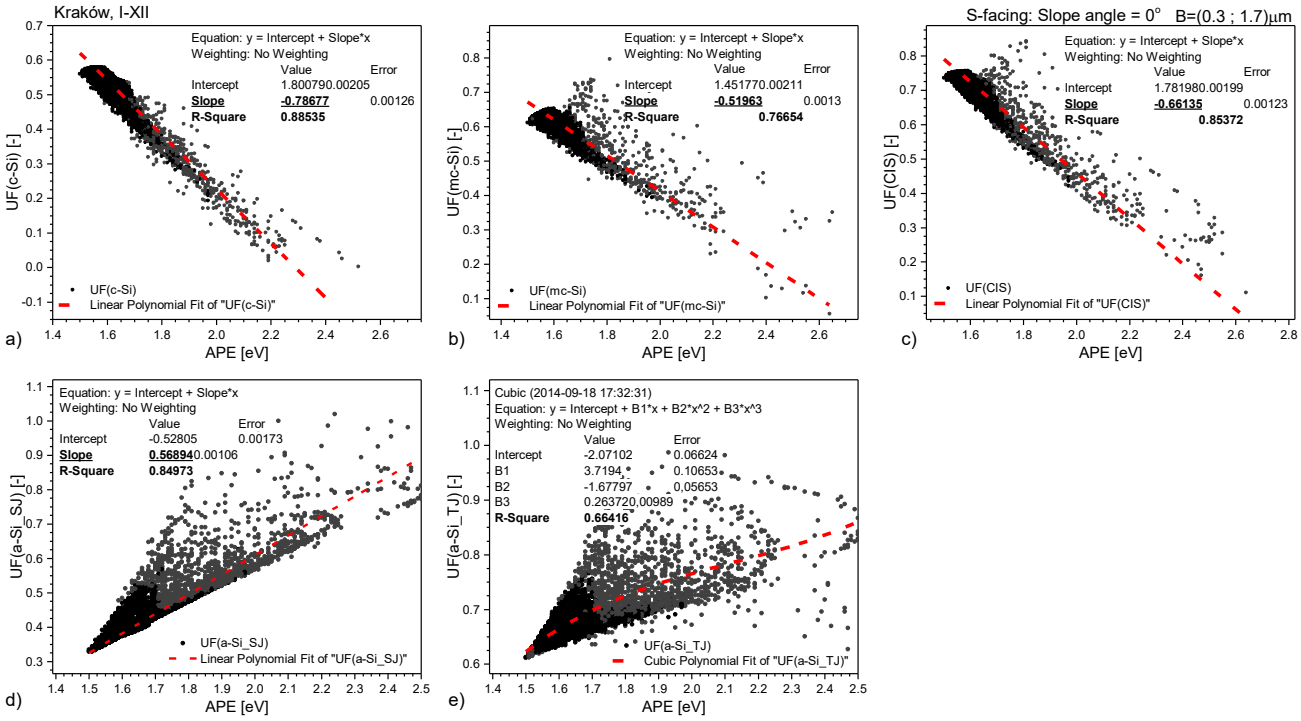

Fig. A2. The influence of *APE* on *UF* content value – of the irradiance falling on the plane of the horizon. The presented results were obtained with reference to band *B*=(0.3; 1.7) µm of the measuring spectroradiometer.

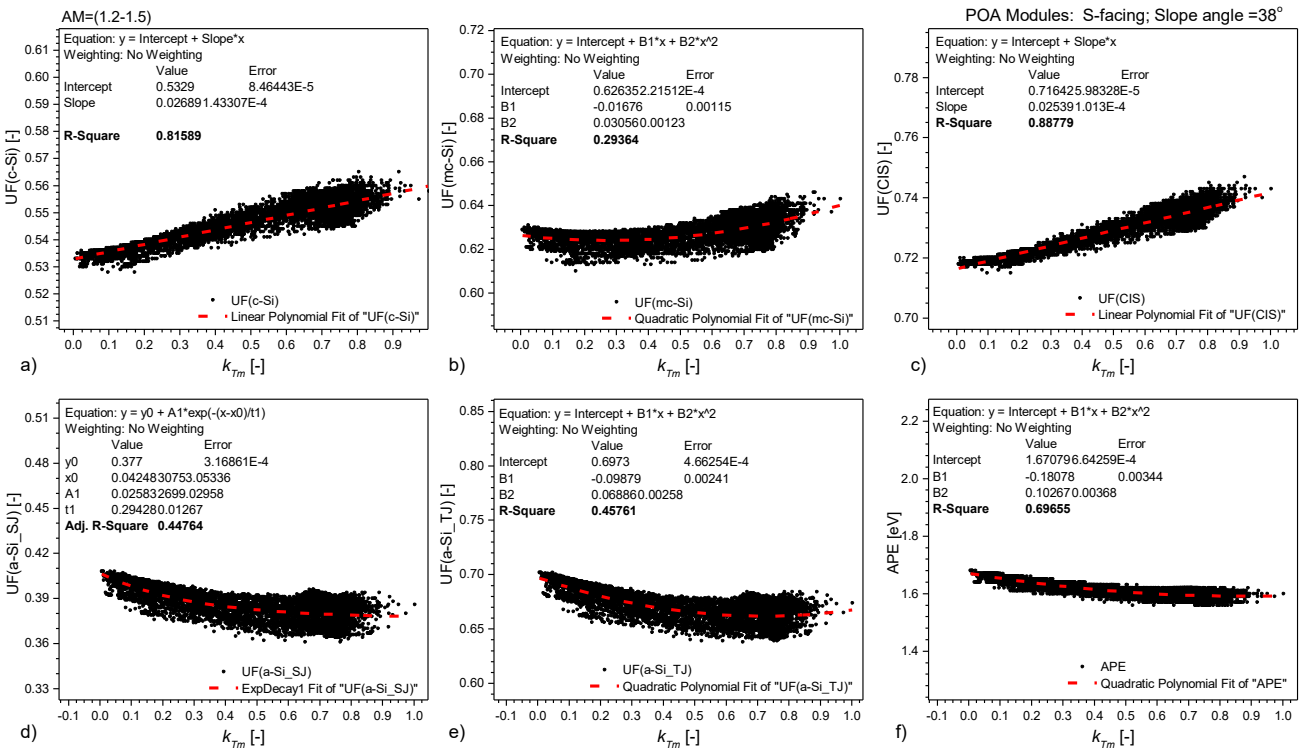

Fig.A3. The influence of clear sky index (k_{Tm}) of irradiance on a–e) content of *UF*, f) value of *APE* – irradiance falling on an optimally inclined plane POA of PV modules. The presented results relate to band *B*=(0.3; 1.7) μm of the measuring spectroradiometer and to the value of air mass from the range *AM*=(1.2; 1.5). The studies were carried out for the city of Kraków.

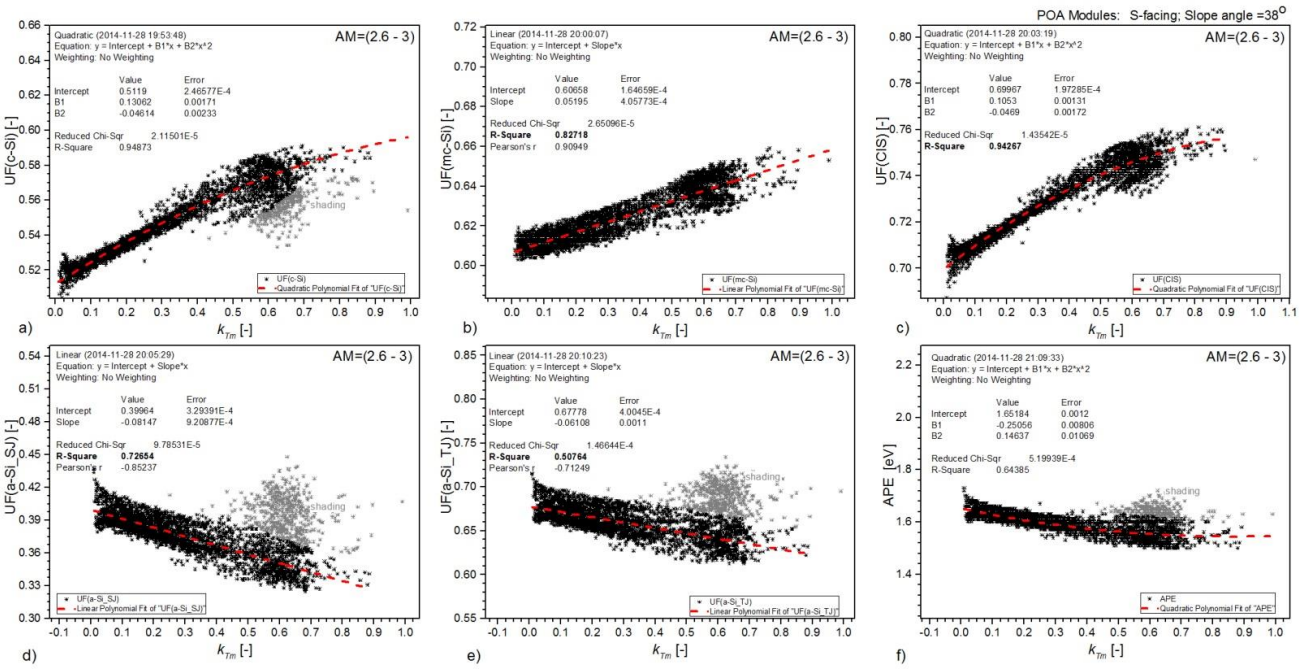

Fig. A4. The influence of clear sky index (k_{Tm}) of irradiance on: a–e) content of *UF*, f) value of *APE* – irradiance falling on an optimally inclined plane POA of PV modules. The presented results relate to band *B*=(0.3; 1.7) μm of the measuring spectroradiometer and to the value of air mass from the range *AM*=(2.6; 3). The studies were carried out for the city of Kraków.

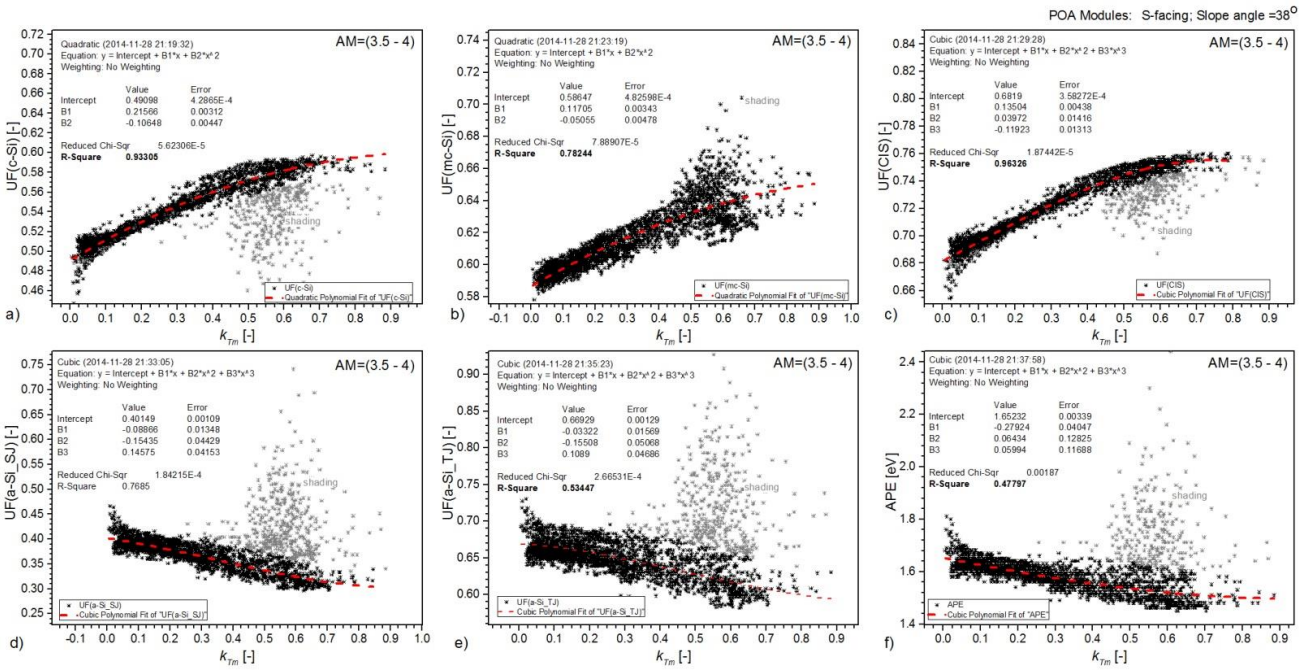

Fig. A5. The influence of clear sky index (k_{Tm}) of irradiance on: a–e) content of UF, f) value of APE – irradiance falling on an optimally inclined plane POA of PV modules. The presented results relate to band B=(0.3; 1.7) μm of the measuring spectroradiometer and to the value of air mass from the range AM=(3.5; 4). The studies were carried out for the city of Kraków.

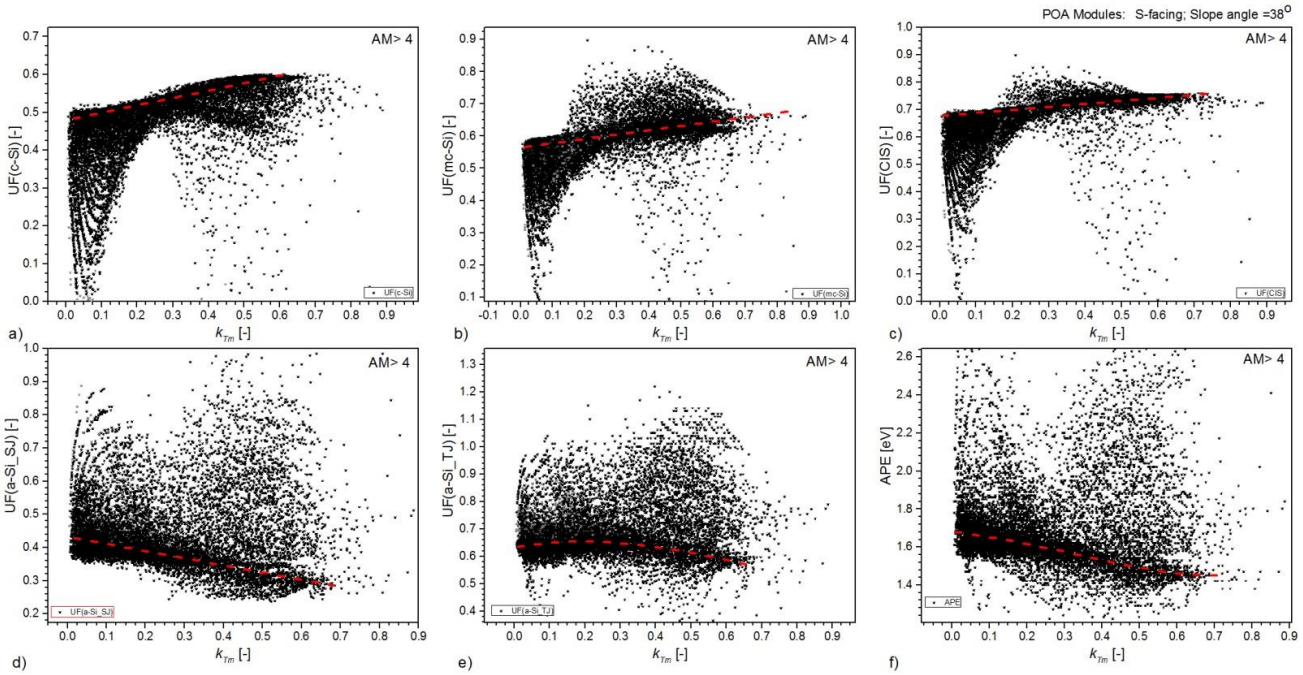

Fig. A6. The influence of clear sky index (k_{Tm}) of irradiance on: a–e) content of *UF*, f) value of *APE* – irradiance falling on an optimally inclined plane POA of PV modules. The presented results relate to band B=(0.3 ;1.7) μm of the measuring spectroradiometer and to the value of air mass from the range AM=(4; 25). The studies were carried out for the city of Kraków.

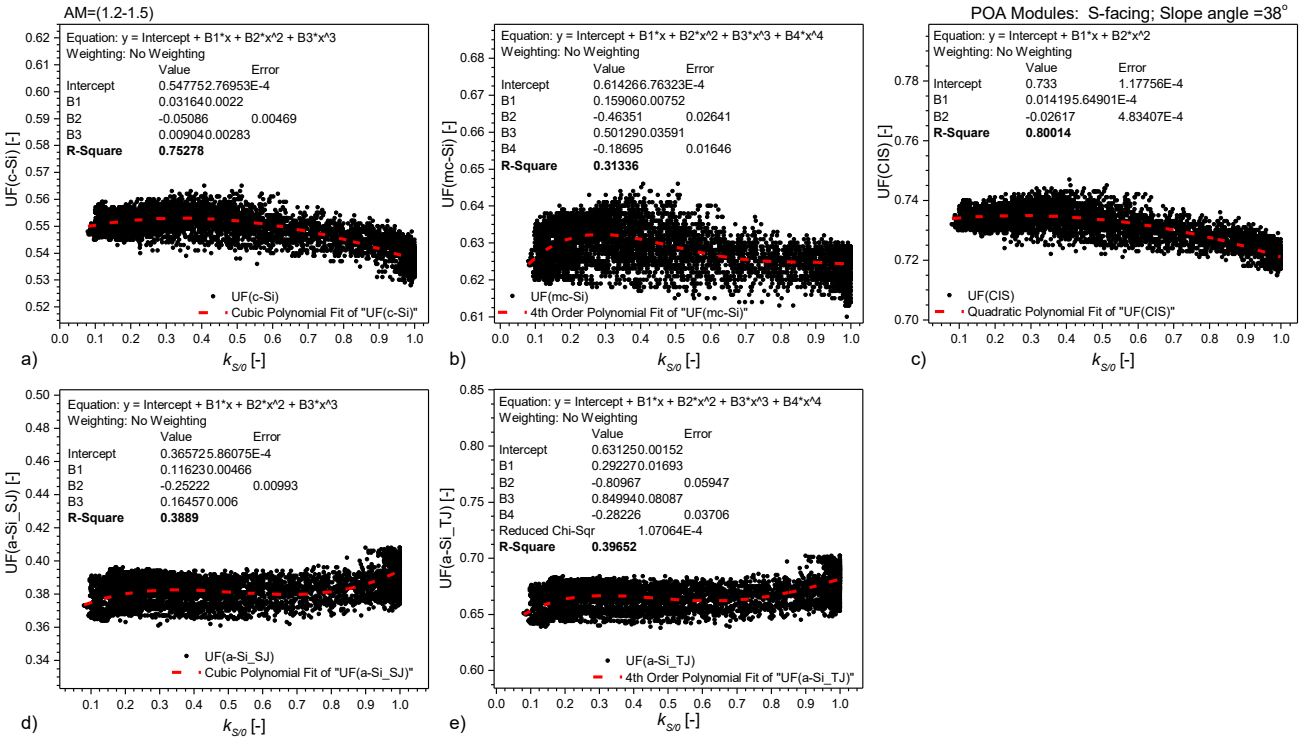

Fig.A7. The influence of the diffused component index value ($k_{s/o}$) of irradiance on a–e) content of *UF*, f) value of *APE* – irradiance falling on an optimally inclined plane POA of PV modules. The presented results relate to band *B*=(0.3; 1.7) μm of the measuring spectroradiometer and to the value of air mass from the range *AM*=(1.2; 1.5). The studies were carried out for the city of Kraków.

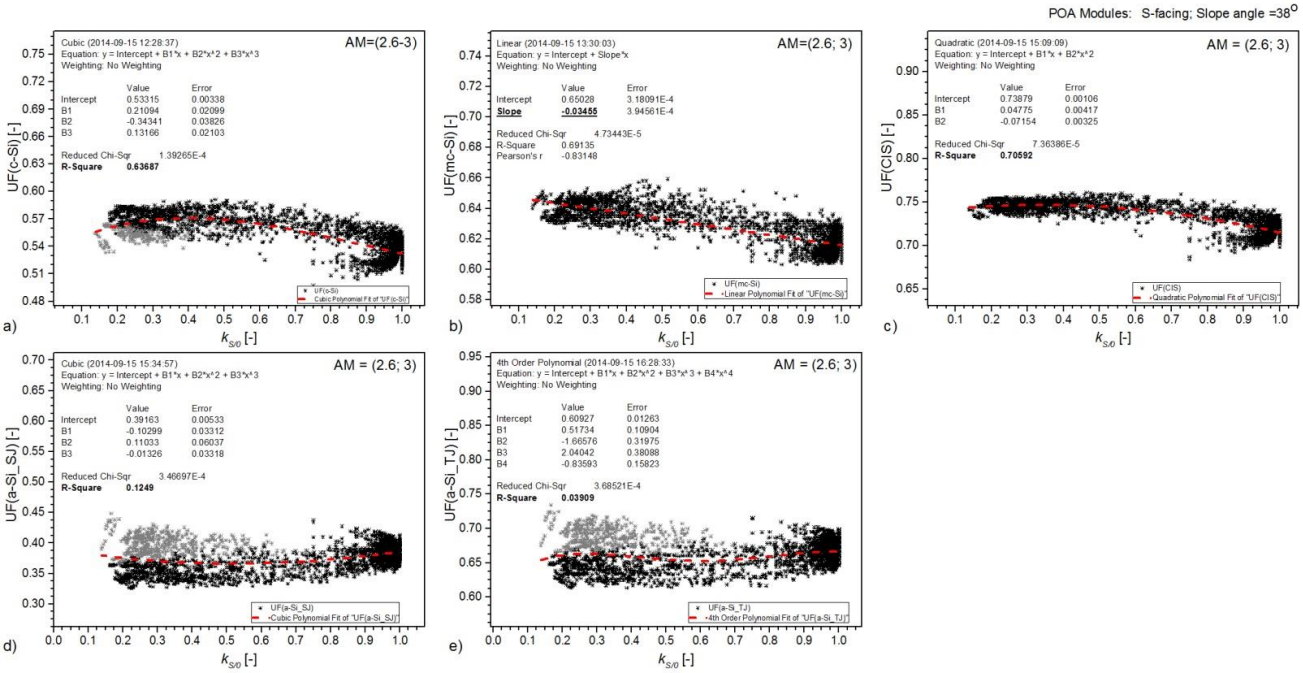

Fig. A8. The influence of the diffused component index value ($k_{s/o}$) of irradiance on: a–e) content of *UF*, f) value of *APE* – irradiance falling on an optimally inclined plane POA of PV modules. The presented results relate to band *B*=(0.3; 1.7) μm of the measuring spectroradiometer and to the value of air mass from the range *AM*=(2.6; 3). The studies were carried out for the city of Kraków.

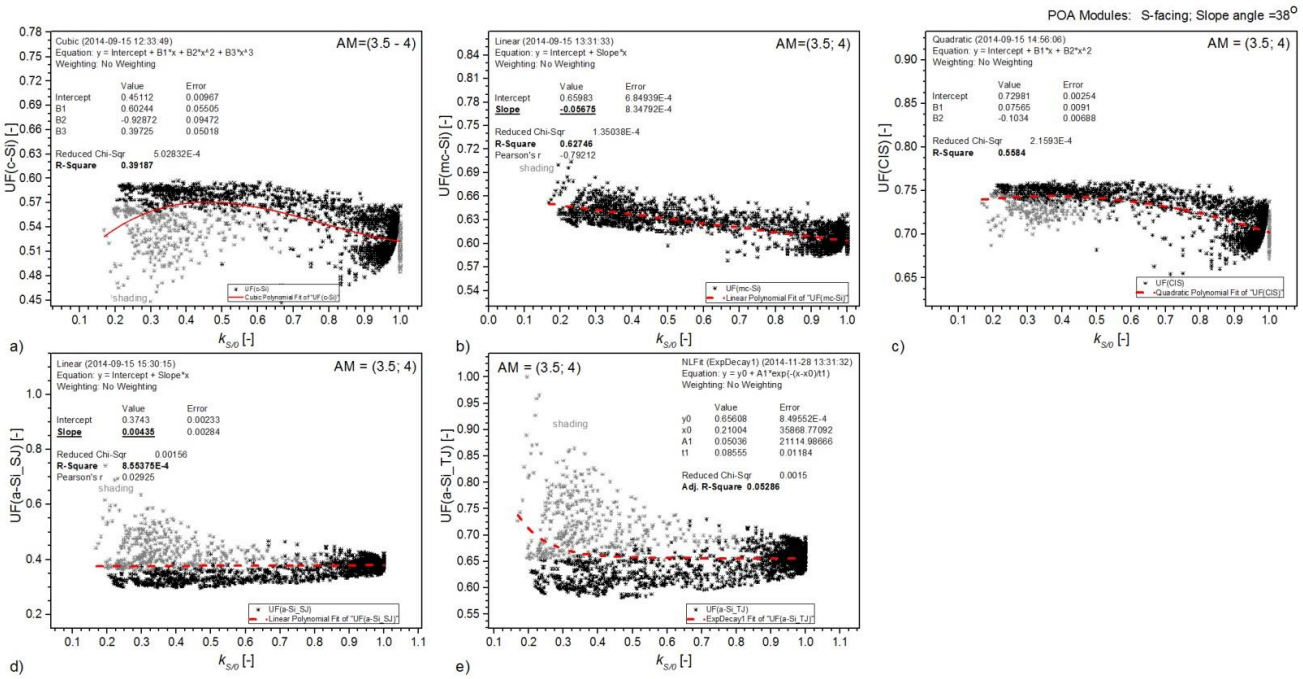

Fig. A9. The influence of the diffused component index value ($k_{s/o}$) of irradiance on: a–e) content of *UF*, f) value of *APE* – irradiance falling on an optimally inclined plane POA of PV modules. The presented results relate to band *B*=(0.3; 1.7) μm of the measuring spectroradiometer and to the value of air mass from the range *AM*=(3.5; 4). The studies were carried out for the city of Kraków.

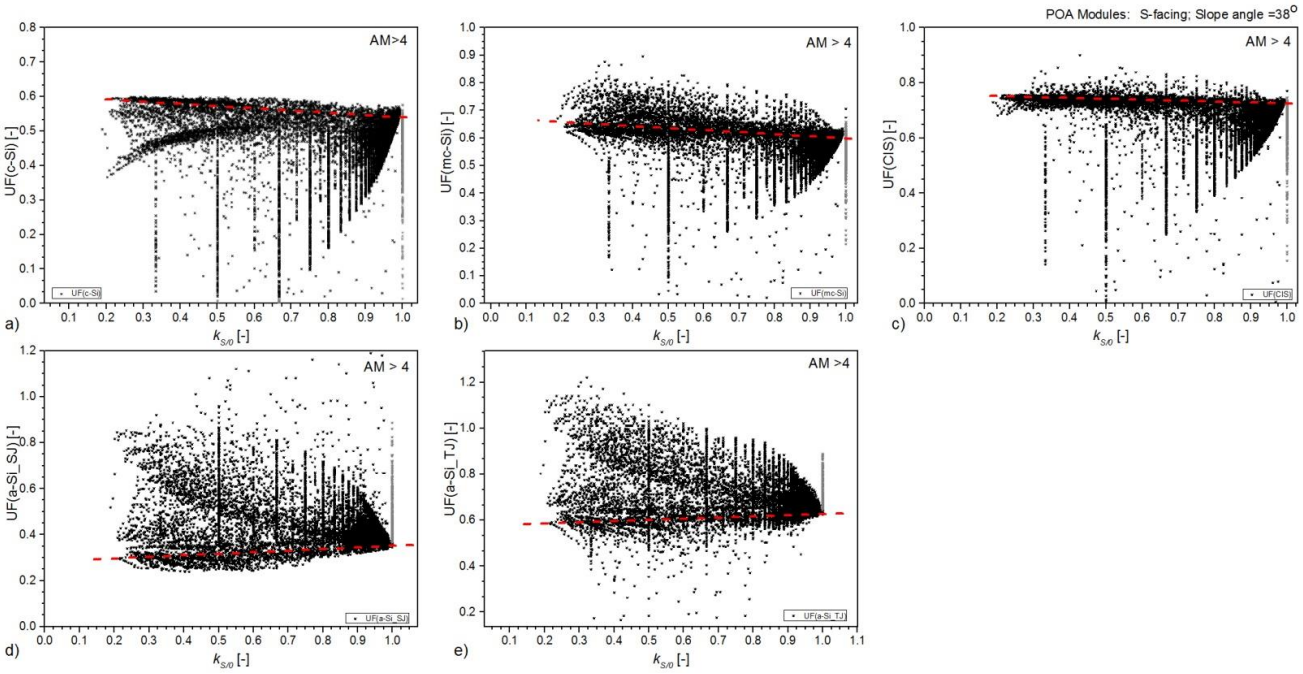

Fig. A10. The influence of the diffused component index value ($k_{s/o}$) of irradiance on: a–e) content of *UF*, f) value of *APE* – irradiance falling on an optimally inclined plane POA of PV modules. The presented results relate to band *B*=(0.3; 1.7) μm of the measuring spectroradiometer and to the value of air mass from the range *AM*=(4; 25). The studies were carried out for the city of Kraków.

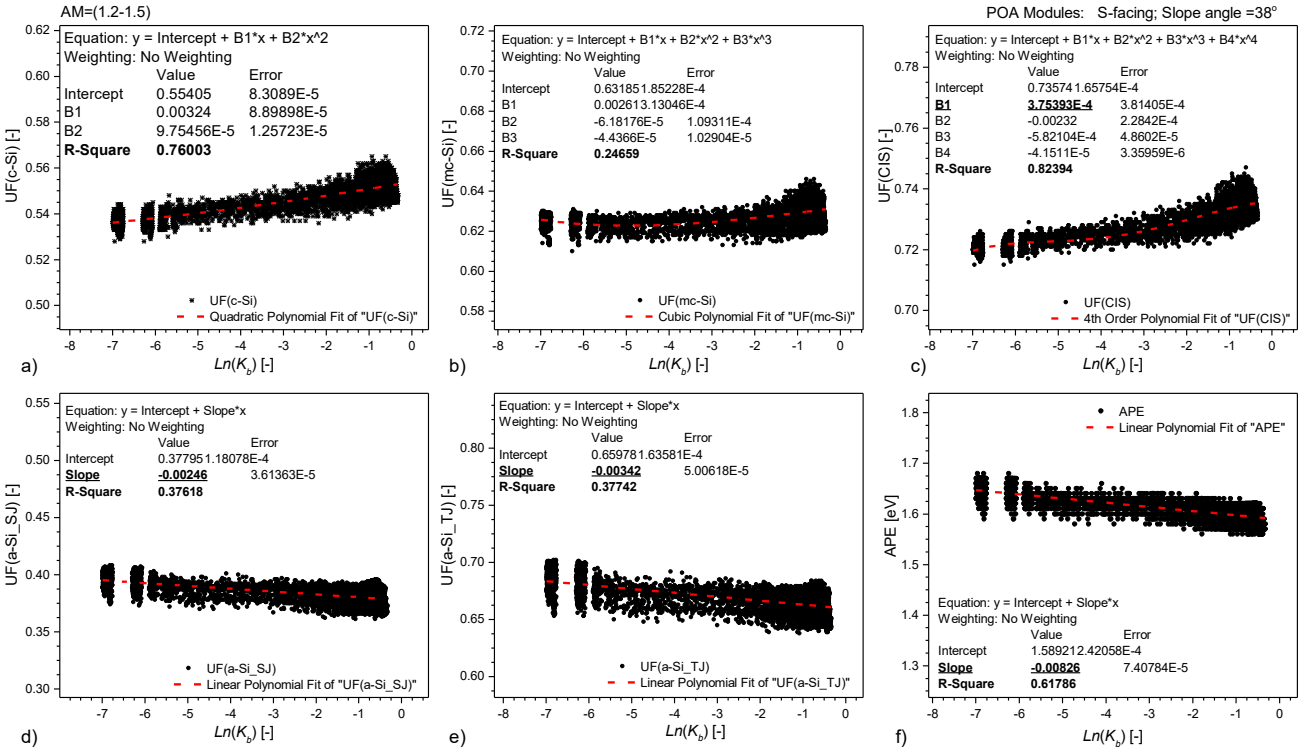

Fig. A11. The influence of the value of logarithm beam clear sky index (K_b) on a–e) content of UF, f) value of *APE* – irradiance falling on an optimally inclined plane POA of PV modules. The presented results relate to band *B*=(0.3; 1.7) μm of the measuring spectroradiometer and to the value of air mass from the range *AM*=(1.2; 1.5). The studies were carried out for the city of Kraków.

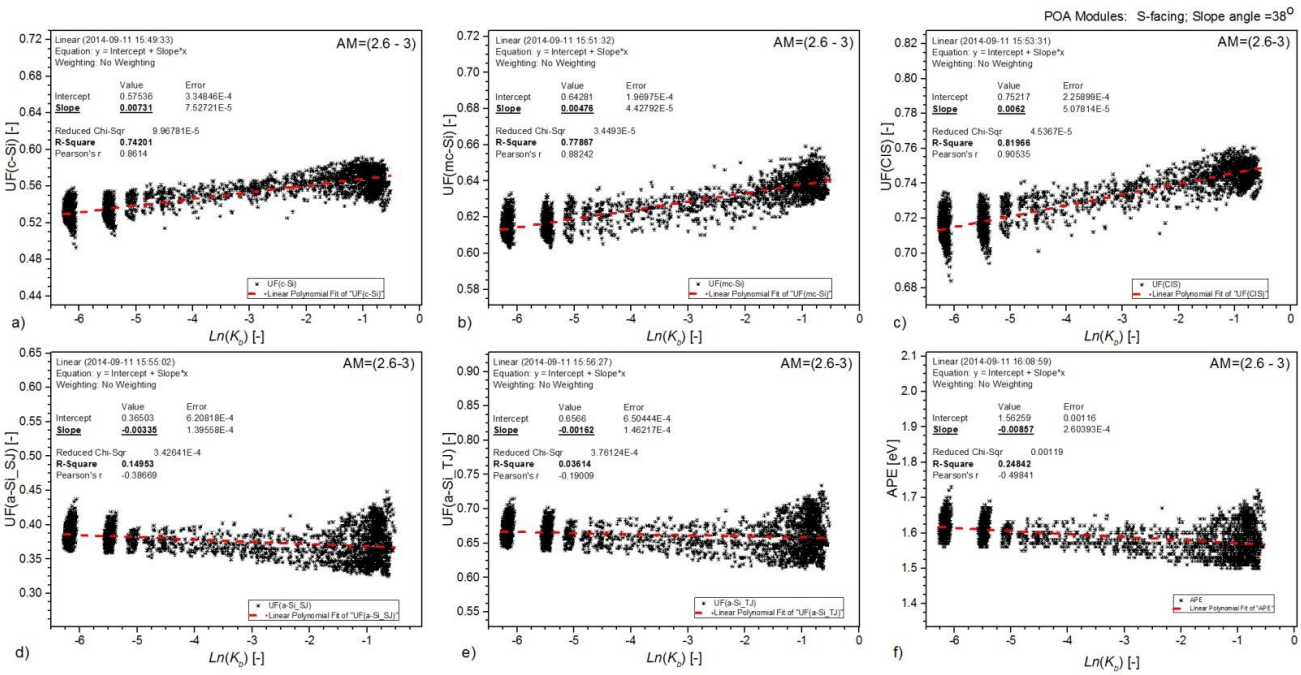

Fig. A12. The influence of beam clear sky index logarithm (K_b) on: a–e) content of *UF*, f) value of *APE* – irradiance falling on an optimally inclined plane POA of PV modules. The presented results relate to band B=(0.3; 1.7) μm of the measuring spectroradiometer and to the value of air mass from the range *AM*=(2.6; 3). The studies were carried out for the city of Kraków.

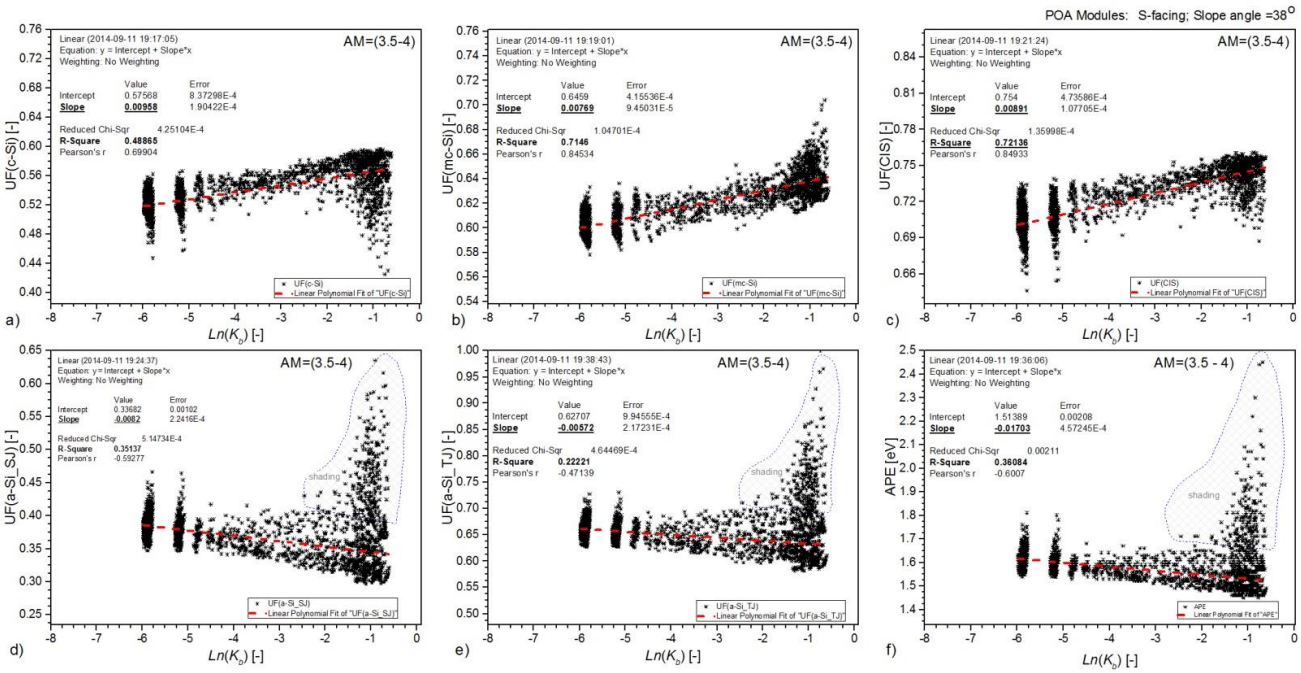

Fig. A13. The influence of beam clear sky index logarithm (K_b) on: a–e) content of *UF*, f) value of *APE* – irradiance falling on an optimally inclined plane POA of PV modules. The presented results relate to band *B*=(0.3; 1.7) μm of the measuring spectroradiometer and to the value of air mass from the range AM=(3.5; 4). The studies were carried out for the city of Kraków.

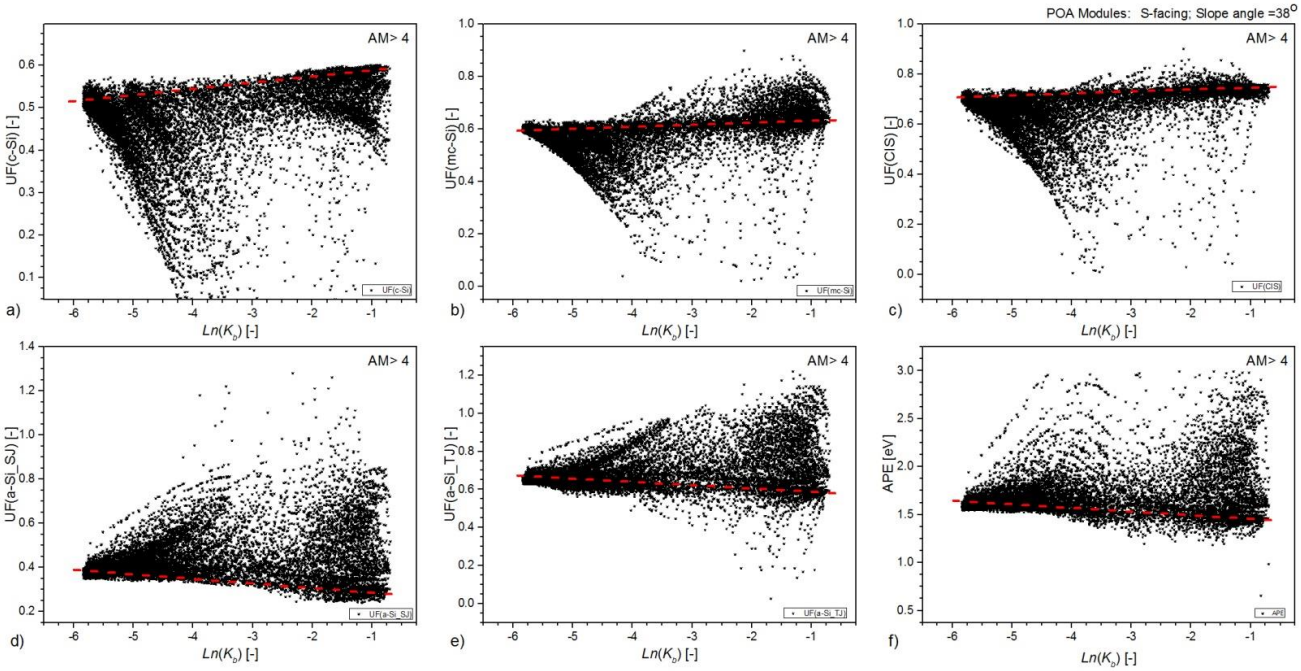

Fig. A14. The influence of beam clear sky index logarithm (K_b) on: a–e) content of *UF*, f) value of *APE* – irradiance falling on an optimally inclined plane POA of PV modules. The presented results relate to band B=(0.3; 1.7) μm of the measuring spectroradiometer and to the value of air mass from the range *AM*=(4; 25). The studies were carried out for the city of Kraków.